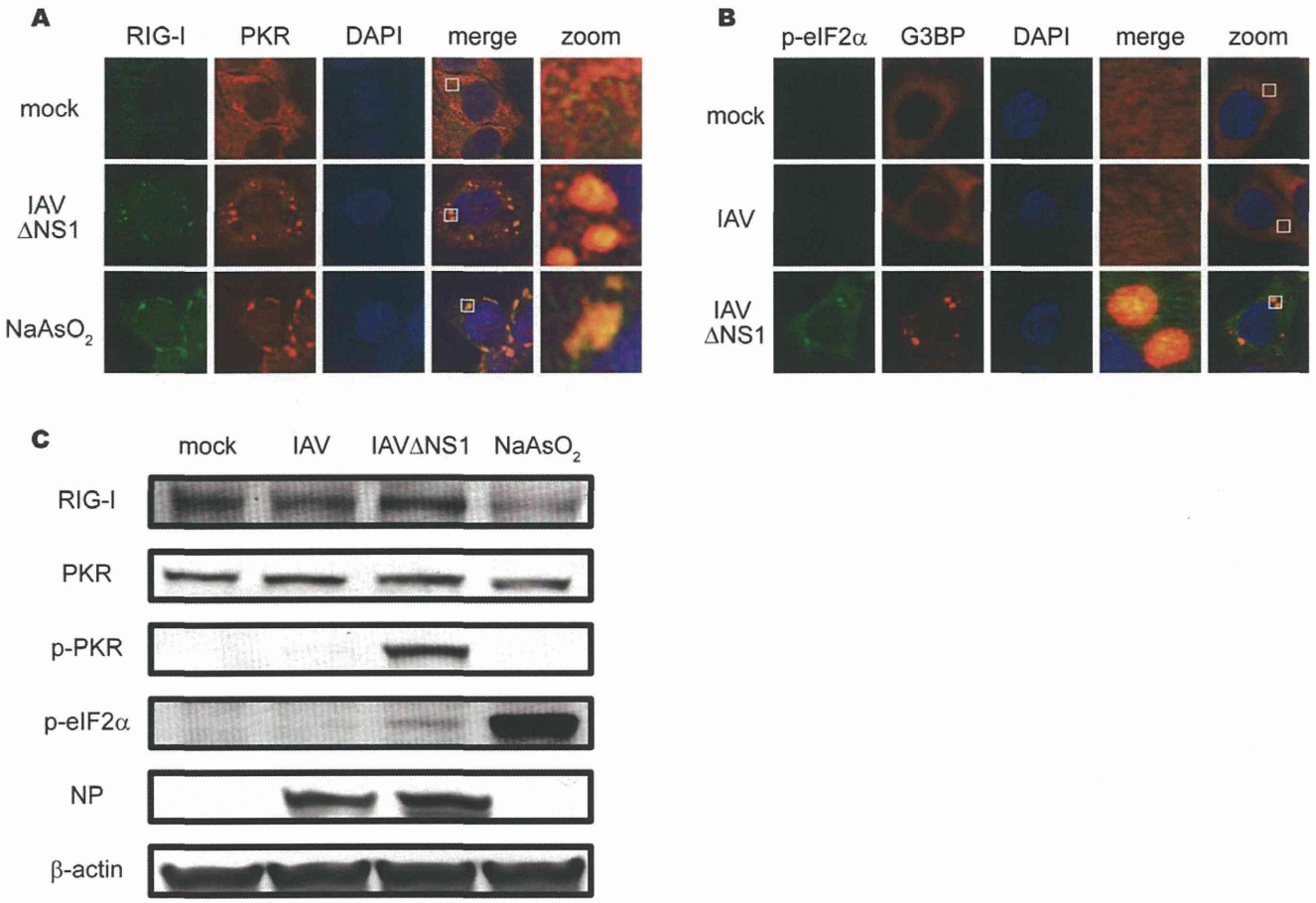

Figure 5. Localization and activation of PKR in IAVÄNS1-induced avSGs. (**A**) HeLa cells were mock-treated or infected with IAVÄNS1 for 9 h or treated with $NaAsO_2$ for 1 h. Cells were fixed and stained with anti-RIG-I and anti-PKR antibodies (% of colocalization: 95.1% and 97.0% in IAVÄNS1-infected and $NaAsO_2$-treated cells, respectively). The zoomed images correspond to the boxed regions. (**B**) HeLa cells were mock-treated or infected with IAV or IAVÄNS1 for 9 h and stained with anti-phospho-eIF2á (Ser 51) (p-eIF2á) and G3BP (% colocalization: 0.0% and 46.5% in IAV and IAVÄNS1-infected cells, respectively). The zoomed images correspond to the boxed regions. (**C**) HeLa cells were infected with IAV or IAVÄNS1 for 12 h or treated with $NaAsO_2$ for 1 h. Cell extracts were prepared and subjected to SDS-PAGE, and immunoblotted using antibodies against RIG-I, PKR, phosphorylated PKR (Thr 446) (p-PKR), phosphorylated eIF2á (Ser 51) (p-eIF2á), IAV NP, and â-actin.
doi:10.1371/journal.pone.0043031.g005

PKR expression, resulting in a strong inhibition of the IAVÄNS1-induced IFN-â gene expression, concomitant impairment of the number of avSG (Figure S6). Taken together, the results indicate that PKR is essential for avSGs and IFN gene activation in IAVÄNS1-infected cells. Importantly, blocking avSG formation by knockdown of PKR or G3BP enhanced the replication of IAVÄNS1 (Figure 7). These results strongly indicate a novel role for avSGs in the antiviral innate immune responses.

It is worth to note that in the absence of PKR, cytoplasmic transport of NP is accelerated (Figure 6A). This effect is also observed in HeLa cells in which PKR is knocked down (Figure S6C). Although the mechanism is unknown, these results suggest that PKR negatively regulate cytoplasmic transport of IAV nucleocapsid.

Viral RNA Generates avSGs in a PKR-dependent Manner

Previous reports showed that genomic RNA of IAV is responsible for triggering antiviral signaling via RIG-I [6,9,24,25]. Because the IAV genome is not infectious, we extracted it from the IAV-infected cells and transfected it into WT or PKR KO MEFs, and investigated whether the IAV genomic RNA solely induces the formation of avSGs and subsequent activation of the IFN gene. As shown in Figure 8A, the IAV genomic RNA is sufficient to produce avSGs, indicating that neither viral protein nor viral RNA replication is required. Furthermore, PKR is required for the formation of viral RNA-induced avSGs (Figure 8A and 8B). Because PKR is also required for poly I:C-induced IFN gene activation [26], we tested short and long poly I:C, which selectively activate RIG-I and MDA5, respectively [27]. Short and long poly I:C induced the formation of avSGs in a PKR-dependent manner (Figure 8A and 8B). We confirmed that IFN-â production by these RNA is PKR-dependent (Figure 8C). Viral but not host RNA is capable of triggering the response, as demonstrated by the finding that total RNA extracted from infected cells but not uninfected cells induced the formation of avSGs and activation of the IFN-â gene (Figure S7A and S7B). These findings demonstrate that PKR is necessary for formation of avSGs which recruits viral RNA and RLRs to trigger IFN gene activation during the IAV-infection. Of note, as shown in Figure 3B, overexpression of PKR can activate SG formation but not IFN expression in the absence of viral RNA, suggesting that function of PKR is prerequisite but insufficient for efficient induction of RLR-mediated antiviral signaling.

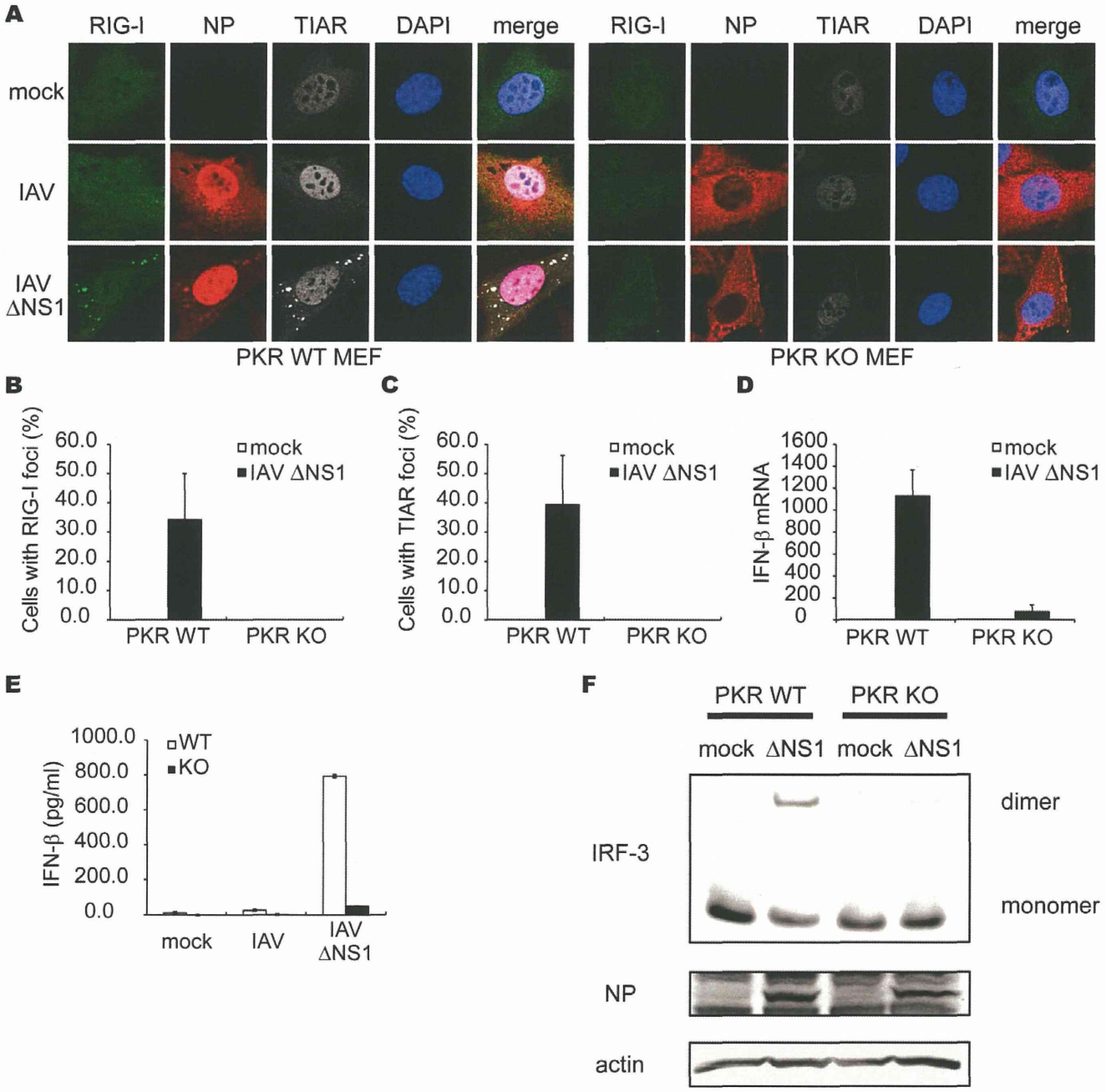

Figure 6. Critical role of PKR in formation of avSG and IFN-â gene activation. (**A–C**) MEFs derived from WT and PKR KO mice were mock-treated or infected with IAVÄNS1 for 12 h. The cells were stained with anti-RIG-I, anti-IAV NP and anti-TIAR antibodies and DAPI (**A**). The percentage of cells containing foci of RIG-I (**B**) or TIAR (**C**) was determined. (**D–F**) PKR WT and PKR KO MEFs were mock-treated or infected with IAVÄNS1. The IFN-â mRNA level at 9 h post-infection was determined by qPCR (**D**). The IFN-â protein levels in culture medium at 15 h post-infection were quantified by ELISA (**E**). Cell extracts were subjected to Native-PAGE and IRF-3 dimer was detected by immunoblotting using anti-IRF-3 antibody. IAV NP and actin were detected by SDS-PAGE followed by blotting using anti-NP and anti-actin antibodies (**F**). Data shown in B-E are represented as the mean standard ± error of the mean (SEM).
doi:10.1371/journal.pone.0043031.g006

Discussion

Recent studies have identified the domain structure of RLRs and the various adaptor proteins regulating RLR-mediated antiviral signaling cascades [28], but how RLRs encounter viral RNA in infected cells remain unclear. In this study, we found that all RLRs are recruited into cytoplasmic granules, termed avSGs, upon viral infections. avSGs contain many SG markers, G3BP, TIAR, and eIF3, but unlike canonical SGs, also contained viral RNA and viral NP. We demonstrated that avSGs are critical to virus-induced IFN gene activation. Since RLRs must efficiently find their ligands to act as vital sensors for viral RNA, avSGs may facilitate a proper encounter between viral RNA and RLRs. In addition, OAS and RNase L are recruited to avSGs, supporting the model that RNase L amplifies IFN-inducing signaling by unearthing cryptic ligands for RIG-I and MDA5 [29]. Further-

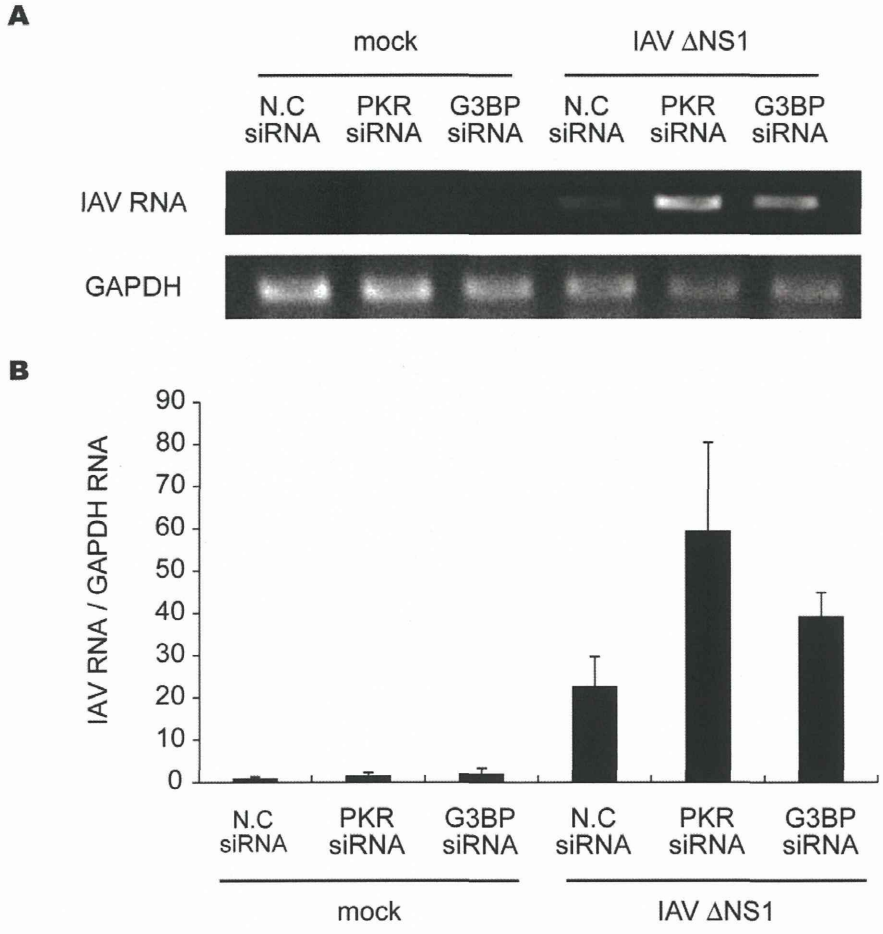

Figure 7. Inhibition of avSG formation enhanced IAV viral replication. HeLa cells were transfected with control siRNA (N.C) or siRNA targeting human PKR mRNA or G3BP. At 48 h after transfection, cells were mock-treated or infected with IAVÄNS1 for 24 h. The expression levels of IAV RNA segment 3 and GAPDH mRNA were determined by RT-PCR (**top**). The IAV RNA expression patterns were quantified with LAS-1000 UV mini (Fujifilm, Japan) and normalized with GAPDH (**bottom**). Data are represented as the mean standard ± error of the mean (SEM).
doi:10.1371/journal.pone.0043031.g007

more, the specific recruitment of antiviral proteins in avSGs suggests a critical role in the blocking of viral replication without an effect on host normal translation. We also observed that other viruses including SINV, EMCV Adenovirus, Hepatitis C virus and Newcastle disease virus induced avSG (Figure S5C and data not shown), suggesting that avSGs may function as a general platform for detection of many viruses to initiate antiviral signaling. Because PKR alone cannot trigger IFN gene activation (Figure 3B), PKR contributes at upstream of IAV-induced RIG-I activation. It was reported that SINV activates GCN2 to phosphorylate eIF2á [30], suggesting that the several viruses may activate different eIF2á kinases to form avSG.

Our model for the function of avSGs is summarized in Figure 9. We do not strictly rule out a possibility that PKR may directly phosphorylate target molecules to participate IFN gene activation, however because activation of PKR alone is not sufficient to trigger IFN production, this effect may be incremental.

Recognition of viral RNA by RIG-I and MDA5 induces ATP-dependent conformational change of the molecules and allows them to interact with mitochondrial IPS-1 via CARD-CARD interaction. Several reports indicated that activated RIG-I forms dimer or oligomer, which is required for efficient signal activation [31,32]. Furthermore, it was demonstrated that IPS-1 is redistributed on mitochondria in response to viral infection and IPS-1 forms prion-like aggregates [12,16]. These observations suggest a possibility that local enrichment of both RLRs and IPS-1 is required for signaling. Although our attempt to detect biochemical interaction between RLR-containing avSG and IPS-1 aggregates *in vitro* has been unsuccessful so far because of insoluble property of them, our immunohistochemical analysis strongly indicates that IPS-1-enriched mitochondria are physically attached with avSG in response to IAVÄNS1 infection (Figure 3E and S4), suggesting critical role of avSG as a platform for RLR-IPS-1 interaction.

The phosphorylation of eIF2á at Ser51 is known to trigger the formation of canonical SGs, however the precise mechanism by which the phosphorylated eIF2á recruits other SG components is not well understood because of difficulty of biochemical analysis [33]. We demonstrated that PKR was activated, recruited to avSGs, and essential for avSGs to form after IAVÄNS1 infection. Viral RNA is primarily responsible for triggering the PKR activation because transfection of IAV genomic RNA or poly I:C induced avSG formation and IFN gene activation in a PKR-dependent manner. Consistent with our data, some studies revealed that PKR deficiency impair production of IFN in response to polyI:C and viral infections [34–38]. Schulz et al. reported that PKR is not required for production of IFN-á/â proteins in response to IAV in bone marrow-derived dendritic cells (BM-DCs) [39]. This is apparently inconsistent with our data

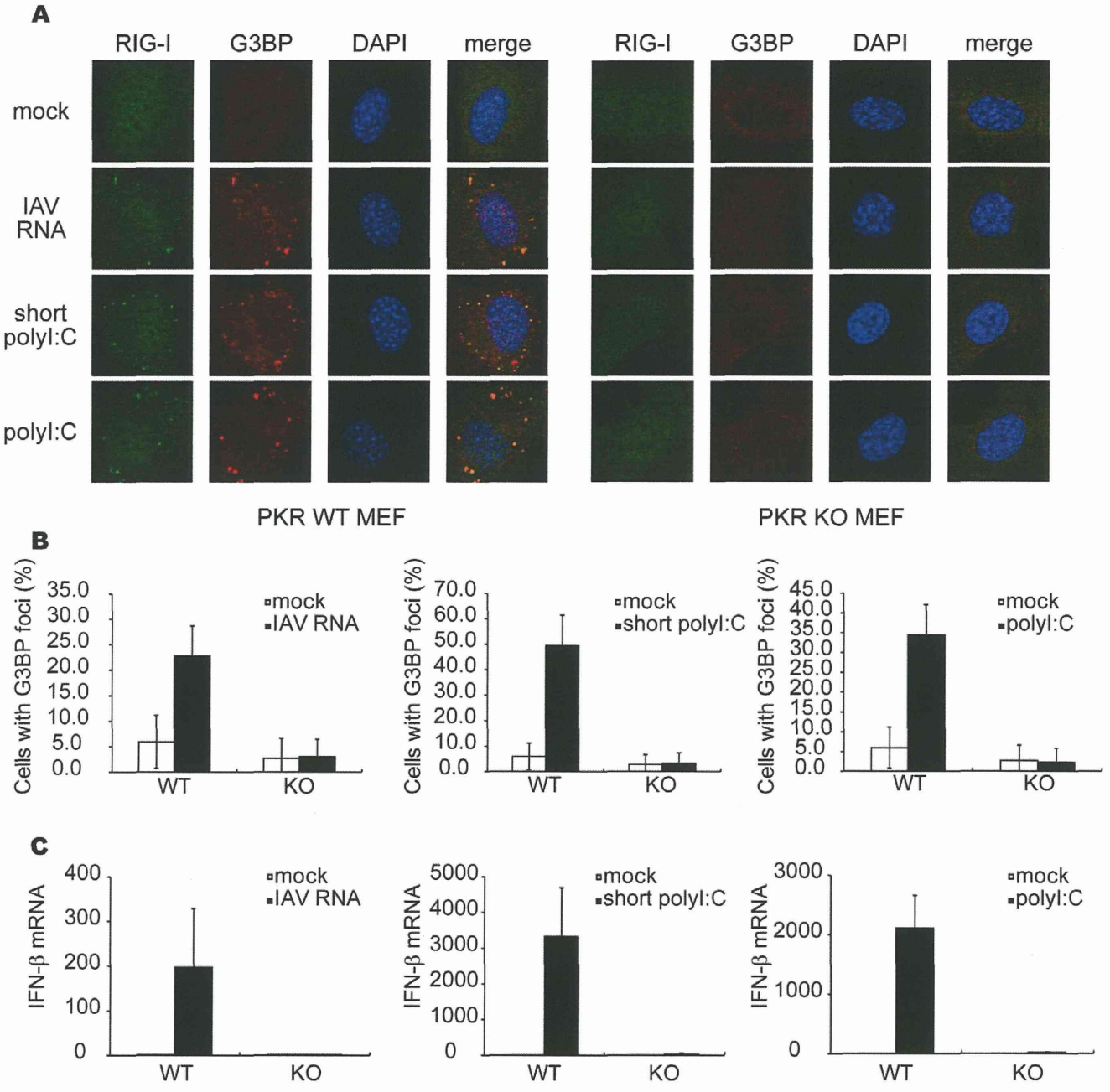

Figure 8. Viral RNA and polyI:C induce formation of avSGs and IFN-â gene expression in a PKR-dependent manner. (**A–C**) MEFs derived from WT and PKR KO mice were mock-treated or transfected with IAV genomic RNA, short poly I:C or long poly I:C for 9 h and stained with anti-RIG-I, anti-G3BP antibodies and DAPI (**A**). The percentage of cells containing foci of G3BP was shown in (**B**). Relative IFN-â mRNA levels were determined by qPCR (**C**). Data shown in B and C are represented as the mean standard ± error of the mean (SEM).
doi:10.1371/journal.pone.0043031.g008

obtained with MEFs. Although we were unable to directly compare between MEF and BM-DC, our explanation for this discrepancy is cell type difference, because IFN protein expression as determined by ELISA (Figure 6E) is consistent with mRNA level (Figure 6D) and PKR knockdown with HeLa cells dramatically diminished IFN production (Figure S6B). BM-DC may utilize eIF2á kinase other than PKR to form avSG.

The NS1 of IAV is a multifunctional protein that inhibits various host factors, including PKR [40,41], RIG-I [42,43], and tripartite motif-containing protein 25 (TRIM25), known to regulate RIG-I activation [44], and potentially sequesters viral dsRNA through its dsRNA-binding domain. Here, we demonstrated that NS1 of IAV markedly inhibited avSGs and the IFN gene's activation. Consistently, a recent report demonstrated that formation of IAV-induced SG was inhibited by wild type NS1, but not by mutant NS1, in which Arg38 and Arg41 are substituted to Ala [41]. Several classes of viruses are known to inhibit the formation of SGs during infection. The West Nile and Sendai viruses encode RNA that interacts with TIAR and inhibits SG assembly [45,46]. The poliovirus 3C protease cleaves G3BP at Gln 326 during the infection process [22]. Moreover, Simpon-Holley et al. recently demonstrated that the E3L protein of Vaccinia virus

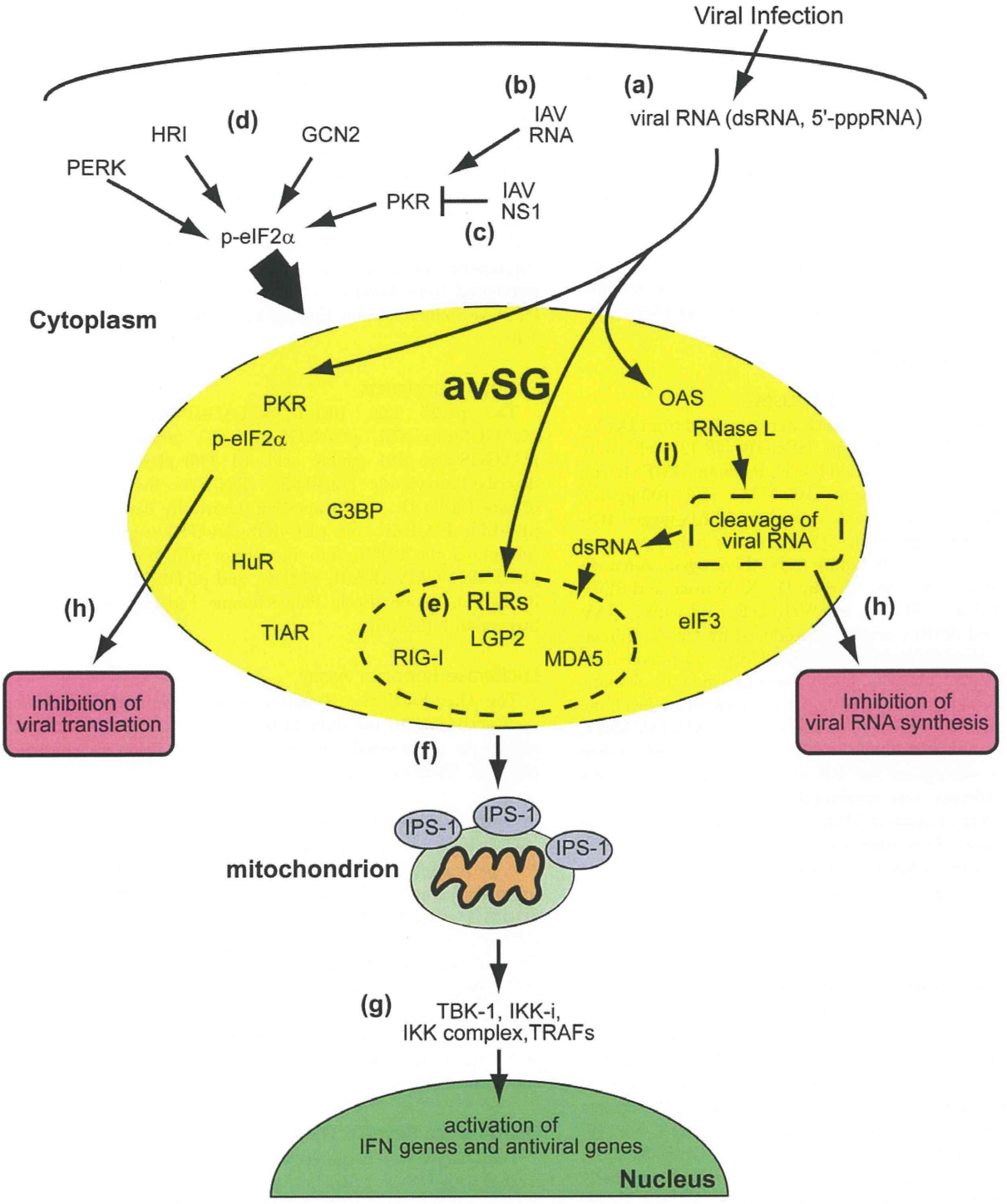

Figure 9. avSGs and innate antiviral responses. Viral infections generate RNA with non-self-signatures such as a 5′-tri-phosphate or double-stranded structure (**a**). In the case of IAVΔNS1, PKR is critical for the formation of avSGs (**b**). Wild-type IAV inhibits formation of avSGs by the actions of the NS1 protein (**c**). Some other viruses may activate different eIF2á kinases, such as GCN2, PERK, and HRI, to produce functional avSGs (**d**). avSGs are composed of SG markers and other RNA-binding proteins including RLRs, antiviral proteins (PKR, OAS, and RNase L) and viral RNA. Within avSGs, viral RNA could be sensed by RLRs to trigger antiviral signaling (**e**). Activated RLRs recruit mitochondrial IPS-1 via CARD-CARD interactions (**f**). IPS-1 serves as another platform for TRAFs and protein kinases, TBK-1, IKKi and IKK complex, to activate target genes (**g**). The antiviral proteins are activated by viral RNA to block viral RNA synthesis and translation (**h**). Moreover, OAS-RNase L system may produce dsRNA to amplify the RLR signaling (**i**).
doi:10.1371/journal.pone.0043031.g009

preventing PKR activation and phosphorylation eIF2á and the Vaccinia virus ÄE3L, lacking E3L genes, generated a granular-like structure distinguished from a granule termed antiviral granule (AVG) [47]. They also reported that MEFs lacking the AVG component TIA-1 exhibited increased Vaccinia viral replication, suggesting that AVG is critical for antiviral host responses. These

results strongly suggest that viruses acquire means to inhibit the formation of avSGs and subsequent activation of the IFN gene.

The canonical SG has been proposed as a storage compartment for translation-stalled host mRNA in response to various stresses and possible partner with another RNP complex, processing body, which is responsible for mRNA degradation [33]. Therefore, SG has been considered as a compartment for dynamic translational regulation upon environmental stress. Our findings discover a new role for newly identified avSG as a platform for interaction between viral RNA and host antiviral molecules to trigger a cascade of events leading to eradication of the virus. Although the difference between SG and avSG is not fully understood at this point, future research will delineate mechanism of their assembly and biological functions in stresses and immune responses.

Materials and Methods

Cell Culture, Transfection, and Viruses

MEFs from *pkr* +/+ and −/− mice were obtained from Dr. Yi-Li Yang [26]. HeLa, 293T, and HEC-1B [48,49] cells were maintained in Dulbecco's modified Eagle's medium (DMEM) with FBS and penicillin-streptomycin (100 U/ml and 100 μg/ml, respectively). HeLa cell line stably expressing FLAG-tagged IPS-1 was described previously [12]. 293T cells were transfected with FuGENE6 (Roche) or Lipofectamine 2000 (Invitrogen). Adenovirus type 12 (Ad12) dl203, provided by Dr. K. Shiroki, and SINV were propagated in 293T cells and Vero cells, respectively. IAV (A/PR/8/34 and ÄNS1), originally produced by Dr. A. Garcia-Sastre (Mount Sinai School of Medicine, USA) and provided by Dr. S. Akira (Osaka University, Japan), were grown in the allantoic cavities of 9-day-old embryonated eggs. Cells were treated with the culture medium ('mock-treated') or infected with IAV, IAVÄNS1, SINV, EMCV, or Ad12 dl203 in serum-free and antibiotic-free medium. After adsorption for 1 h at 37°C, the medium was changed and infection was continued for various periods in the presence of serum-containing DMEM. IAV genomic RNA was extracted from partially purified virus stock by TRIzol (Invitrogen) and 1.0 μg of viral RNA was transfected with Lipofectamine RNAi MAX (Invitrogen) in a 35 mm dish. PolyI:C was purchased from Amersham. Short polyI:C was prepared as described previously [27].

Immunoblotting, Antibodies and Reagents

The preparation of cell extracts and immunoblotting have already been described previously [5,50]. The polyclonal antibody used to detect human IRF-3 in native PAGE and anti-human and anti-mouse IRF-3 polyclonal antibodies for immunostaining were described previously [50]. The monoclonal antibody against Influenza NP (mAb61A5), which was generated by Dr. Y. Kikuchi (Iwaki Meisei University, Japan), was provided by Dr. F. Momose (Kitasato University, Japan) [51]. The monoclonal antibody against human OAS (6-1) was provided by Dr. Y. Sokawa (Kyoto Institute of Technology, Japan). The anti-human RIG-I, anti-human MDA5, and anti-human LGP2 antibodies were originally generated by immunizing rabbits with a synthetic peptide corresponding to amino acids 793–807 of human RIG-I, 145–160 of human MDA5, and 535–553 of human LGP2, respectively. As shown in Figure S1, knockdown of endogenous RIG-I by shRNAs specifically inhibit granule-like accumulation of RIG-I in immunostaining (Figure S1A) and appearance of band corresponding endogenous RIG-I in western blotting (Figure S1B), indicating high specificity of the anti-RIG-I antibody. Furthermore, a similar staining pattern was obtained with a monoclonal antibody for human RIG-I produced by Perseus Proteomics Inc, Japan. Other antibodies were obtained from the following sources: anti-G3BP (611126) from Transduction Laboratories™, anti-IRF-3 (CBX00167) from COSMO BIO, anti-PKR (sc-6282), anti-RNase L (sc-22870), anti-G3BP (sc-70283), anti-eIF3 (sc-16377), anti-c-myc (sc-40) and anti-TIAR (sc-1749) from Santa Cruz Biotechnology, anti-FLAG (M2) from Sigma, anti-phospho-PKR (pT446) (1120-1) from Epitomics, anti-actin (MAB1501R) from CHEMICON International, anti-PMP70 (ab3421) from Abcam, anti-HA-Tag (6E2) and anti-phospho-eIF2á (Ser51) (119A11) from Cell Signaling, and anti-HuR (RN004P, RIP-Certified antibody) and anti-â-actin (PM053) from MBL. Alexa 488-, 594-, and 633-conjugated anti-mouse, anti-rabbit, or anti-goat IgG antibodies purchased from Invitrogen were used as secondary antibodies. 0.5 mM Sodium arsenite (Sigma) was added to the cell culture for 1 h.

Plasmid Constructs

The p-125 Luc, pEF-BOS-FLAG-IPS-1, pCAGGS-myc, pCAGGS-myc-NS1, pCAGGS-myc-NS1 (amino acids 1–80), pCAGGS-myc-NS1 (amino acids 81–230) plasmids have been described previously [42,48,52]. cDNA for human PKR was obtained from Dr. A. Hovanessian (University Paris, France) and pEF-BOS-HA-PKR and pEF-BOS-HA-IPS1 were obtained by subcloning the cDNA into the vector pEF-BOS, respectively. pSUPER, pCMVÄR8.91, pMDG, and pRDI292 were provided by Dr. D. Trono (Ecole Polytechnique Federale de Lausanne, Switzerland) [53–56].

Luciferase Reporter Assay

The Dual-Luciferase Reporter Assay System (Promega) was used according to the manufacturer's instructions for luciferase assays. As an internal control, the *Renilla* Luciferase construct pRL-TK (Promega) was used.

Immunofluorescence Microscopy

Cells were fixed with 4% paraformaldehyde (PFA) for 20 min at 4°C, permeabilized with 0.05% Triton X-100 in PBS for 5 min at room temperature (RT), blocked with 5 mg/ml BSA in PBST (0.04% Tween20 in PBS) for 30 min, and incubated with relevant primary antibodies diluted in blocking buffer overnight at 4°C. The cells were then incubated with secondary antibodies for 1 h at RT. Nuclei were stained with 4.6-dimaidino-2-phenylinodole (DAPI) and analyzed with a confocal laser microscope, LSM 510-V4.2 (Carl Zeiss) or TCS-SP (Leica). The percentages of avSG-containing cells were calculated in more than 5 randomly chosen fields for each slide.

Quantitative Reverse Transcription-PCR

Total RNA was prepared with TRIzol reagent (Invitrogen), treated with DNase I (Roche Applied Science), and amplified by reverse transcription-PCR with the ABI PRISM 7700 sequence detection system (Applied Biosystems). TaqMan reverse transcription reagents (Applied Biosystems) were used for cDNA synthesis. We used commercial TaqMan Universal PCR Master Mix and TaqMan primer-probe sets (Applied Biosystems) for human and mouse IFN-â. As an internal control for the comparative threshold cycle methods, a primer-probe set for eukaryotic 18 s rRNA (Applied Biosystems) was used. The results were normalized to the abundance of internal control. For the detection of IAV RNA and glyceraldehyde-3-phophate dehydrogenase (GAPDH), we used specific primer sets and amplified with Ex Taq HS (Takara). IAV RNA: 5¢- ATTTGCAACACTACAGGGGC-3¢ (forward) and

5¢-GACTGACGAAAGGAATCCCA-3¢ (reverse). GAPDH mRNA:

5¢- GAGTCAACGGATTTGGTCGT-3¢ (forward) and

5¢- TTGATTTTGGAGGGATCTCG-3¢ (reverse).

Co-immunoprecipitation

The RIG-I antibody was cross-linked to Dynabeads protein G (Invitrogen) according to the manufacturer's protocol. Cell lysate was incubated with the anti-RIG-I antibody -Dynabeads for 120 min at RT. RIG-I-immunoprecipitated complexes were eluted by boiling in loading buffer and then processed for Western blotting.

RNA Interference

A lentiviral shRNA expression system was used. RIG-I shRNA#1 and RIG-I shRNA#2 were originally constructed. Oligonucleotides with the following sense and antisense sequences were used for the construction of the small hairpin RNA (shRNA)-encoding lentiviral vector. RIG-I shRNA#1; 5¢-GATCCCC-GAGGTGCAGTATATTCAGGTT CAAGAGACCTGAATA-TACTGCACCTCTTTTTGGAAA-3¢ (sense) and 5¢-AGCTT T TCCAAAAAGAGGTGCAGTATATTCAGGTCTCTT-GAACCTGAATATACTG CACCTCGGG-3¢ (antisense). RIG-I shRNA#2; 5¢-GATCCCCGAATTTAAAACCA GAAT-TATCTTCAAGAGAGATAATTCTGGTTT-TAAATTCTTTTTGGAAA-3¢ (sense) and 5¢-AGCTTTTC-CAAAAAGAATTTAAAACCAGAATTATCTCTC TTGAA-GATAATTCTGGTTTTAAATTCGGG-3¢ (antisense). The oligonucleotides described above were annealed and subcloned into the Bgl II-Hind III site of pSUPER. To construct the pLV-shRNA against RIG-I, the BamHI-SalI fragments excised from pSUPER-RIG-I#1 and pSUPER-RIG-I#2 were subcloned into the BamHI-SalI site of pRDI292. The recombinant lentiviruses were generated by transfection of the empty lentiviral vector, or respective shRNA construct together with the packaging construct pCMVÄR8.91 and the envelop plasmid pMDG. At 48 h after, the culture supernatant was collected and the medium filtered with a 0.45-μm filter was transferred, to HeLa cells. After 72 h, the cells were selected with medium containing 2 μg/ml of Puromycin (Sigma). The siRNA negative control and siRNAs targeting PKR and G3BP were purchased from Invitrogen. Each siRNA was transfected with Lipofectamine RNAi MAX (Invitrogen) according to the manufacturer's instructions. At 48 h post-transfection, cells were harvested, infected with IAVÄNS1, and then subjected to Real Time PCR, immunofluorescence assays, or SDS-PAGE followed by immunoblotting.

Fluorescence in situ Hybridization (FISH) Assay

FISH assays have been described previously [57]. Briefly, after the immunofluorescence assays, cells were fixed in 4%PFA for 10 min and permeablized on ice with 0.5% Triton X-100 in PBS for 5 min. After deproteinization by Proteinase K, cells were re-fixed in 4% PFA for 10 min and then subjected to stepwise dehydration in ethanol. The dried coverslips were incubated with a biotin-labeled RNA probe for 12 h at 37°C. After hybridization, cells were washed and incubated with avidin-FITC for 30 min at 37°C. Nuclei were stained with TO-PRO-3 and examined by confocal laser-scanning microscope.

Enzyme-linked Immunosorbent Assay (ELISA)

Culture supernatants were collected and subjected to ELISA with mouse IFN-â kit (PBL Interferon Source) according to the manufacturers' instructions.

Supporting Information

Figure S1 Anti-RIG-I antibody specifically recognizes endogenous human RIG-I. HeLa cells were infected with control lentivirus or two lentiviruses encoding different RIG-I-specific shRNAs (#1 and #2) for 72 h. **(A)** The cells were treated with $NaAsO_2$ for 1 h and stained for RIG-I and G3BP. $NaAsO_2$ induces speckle-like localization of RIG-I and G3BP. **(B)** The cells were treated with human IFN-â for 12 h. Cell extracts were prepared and subjected to SDS-PAGE, and immunoblotted using antibodies against RIG-I, MDA5, and â-actin. The RIG-I signals were diminished by knockdown of RIG-I.
(TIF)

Figure S2 N-terminal region of NS1 is sufficient to block RIG-I aggregation and antiviral signals. (A) 293T cells were transfected with empty vector (empty), myc-tagged NS1 (myc-NS1 (Full)), N-terminal NS1 (1–80), or C-terminal NS1 (81–230) for 48 h. The cells were mock-treated (mock) or infected with IAVÄNS1 for 9 h and stained for RIG-I and NS1 (myc). The percentage of cells with IAVÄNS1-induced RIG-I speckle was 0.0%, 2.3%, 43.1%, for NS1, NS1 (1–80), and NS1 (81–230)-expressing cells, respectively. **(B)** 293T cells were transiently transfected with reporter plasmids containing natural IFN-â promoter together with the indicated NS1-expressing vectors. Transfected cells were mock-treated or infected with IAVÄNS1 for 12 h and subjected to the Dual-Luciferase assay. Data are presented as the mean standard ± error of the mean (SEM).
(TIF)

Figure S3 Localization of Viral RNA in IAV-infected cells. (A and B) HeLa cells were mock-treated or infected with IAV for 12 h. Viral RNA (vRNA) was detected by the FISH method using an RNA probe complementary to the segment 1 of IAV and NP **(A)** and RIG-I **(B)** were detected using anti-NP and anti-RIG-I antibodies. TO-PRO-3 was used for staining of nuclear DNA (DNA). Viral RNA and NP did not form foci.
(TIF)

Figure S4 IPS-1 was accumulated in close proximity to the RIG-I foci. HeLa cells stably expressing FLAG-tagged IPS-1 were mock-treated or infected with IAV or IAVÄNS1 for 10 h. The cells were stained with anti-FLAG and anti-RIG-I antibodies and DAPI. The merged images of FLAG and RIG-I are enlarged in the bottom panel. The white arrowheads indicate RIG-I/IPS-1 contacts. These contacts were observed in 74.2% and 1.8% of IAVÄNS1- and IAV-infected cells, respectively.
(TIF)

Figure S5 avSG formation is not a consequence of IFN gene activation. (A) 293T cells were transfected with empty vector or the expression vector for IPS-1 (HA-IPS-1) for 24 h. Cells were stained for IRF-3, HA-tag and TIAR. Nuclear IRF-3 was observed in almost all of the IPS-1-expressing cells (95.5%), however these cells exhibited little foci of TIAR (3.0%). **(B)** HEC-1B cells deficient for type I IFN receptor were mock-treated, infected with IAVÄNS1 for 9 h, or treated with $NaAsO_2$ for 1 h as indicated. Cells were stained for RIG-I and G3BP. SGs and avSGs were observed in HEC-1B cells (% colocalization 98.4% and 92.9% for IAVÄNS1 and $NaAsO_2$, respectively). The zoomed images correspond to the boxed regions. **(C)** HeLa cells were mock-treated or infected with SINV, EMCV, or Ad12 dl203 for 9 h, fixed, and stained for RIG-I and G3BP as indicated (% colocalization: 99.2%, 98.4%, and 98.2%, respectively). The zoomed images correspond to the boxed regions.
(TIF)

Figure S6 IAV-induced formation of avSGs was inhibited in PKR knockdown cells. (A–E) HeLa cells were transfected with control siRNA (N.C) or siRNA targeting three independent parts of human PKR mRNA (#1 3). **(A)** At 48 h after transfection, cells were harvested and PKR and actin were detected by Western blotting. **(B–E)** At 48 h after transfection, cells were mock-treated (open bar) or infected with IAVÄNS1 (filled bar) for 9 h. The level of IFN-â mRNA was determined by qPCR **(B)**. Immunostaining of HeLa cells transfected with control (N.C) or PKR-targeted (PKR) siRNA after mock-treatment or infection with IAVÄNS1 **(C)**. Cells were also examined by staining for foci of RIG-I **(D)**, TIAR **(E)** after 12 h infection. Percentages of cells containing the respective foci are indicated. Data are presented as the mean standard ± error of the mean (SEM).
(TIF)

Figure S7 Total RNA from IAV-infected cells but not uninfected cells induces avSG formation and IFN-â gene activation. (A and B) Wild-type MEF were mock-treated (no RNA) or transfected with total RNA extracted from uninfected MEFs (MEF RNA) or from IAV-infected cells for 12 h (IAV infected MEF RNA). The cells were stained for RIG-I and G3BP (% avSG formation 0.0%, 4.0%, and 21.4% for no RNA, MEF RNA, and IAV infected MEF RNA, respectively) **(A)**. The zoomed images correspond to the boxed regions. Endogenous IFN-â mRNA levels were determined by qPCR **(B)**. Data are presented as the mean standard ± error of the mean (SEM).
(TIF)

Acknowledgments

We thank R. Kageyama for making their confocal microscope available for this study, F. Momose and Y. Kikuchi for the anti-IAV NP antibody, and Y. Sokawa for the anti-OAS antibody.

Author Contributions

Conceived and designed the experiments: KO MY TF. Performed the experiments: KO MJ JY RN SM AT AK SO TM. Analyzed the data: KO KN HN MY TF. Contributed reagents/materials/analysis tools: SS. Wrote the paper: KO MY TF.

References

1. Samuel CE (2001) Antiviral actions of interferons. Clin Microbiol Rev 14: 778–809, table of contents.
2. Witte K, Witte E, Sabat R, Wolk K (2010) IL-28A, IL-28B, and IL-29: promising cytokines with type I interferon-like properties. Cytokine Growth Factor Rev 21: 237–251.
3. Gale M Jr, Katze MG (1998) Molecular mechanisms of interferon resistance mediated by viral-directed inhibition of PKR, the interferon-induced protein kinase. Pharmacol Ther 78: 29–46.
4. Rubinstein S, Familletti PC, Pestka S (1981) Convenient assay for interferons. J Virol 37: 755–758.
5. Yoneyama M, Kikuchi M, Natsukawa T, Shinobu N, Imaizumi T, et al. (2004) The RNA helicase RIG-I has an essential function in double-stranded RNA-induced innate antiviral responses. Nat Immunol 5: 730–737.
6. Kato H, Takeuchi O, Sato S, Yoneyama M, Yamamoto M, et al. (2006) Differential roles of MDA5 and RIG-I helicases in the recognition of RNA viruses. Nature 441: 101–105.
7. Yoneyama M, Kikuchi M, Matsumoto K, Imaizumi T, Miyagishi M, et al. (2005) Shared and unique functions of the DExD/H-box helicases RIG-I, MDA5, and LGP2 in antiviral innate immunity. J Immunol 175: 2851–2858.
8. Hornung V, Ellegast J, Kim S, Brzozka K, Jung A, et al. (2006) 5′-Triphosphate RNA is the ligand for RIG-I. Science 314: 994–997.
9. Pichlmair A, Schulz O, Tan CP, Naslund TI, Liljestrom P, et al. (2006) RIG-I-mediated antiviral responses to single-stranded RNA bearing 5′-phosphates. Science 314: 997–1001.
10. Rasmussen SB, Jensen SB, Nielsen C, Quartin E, Kato H, et al. (2009) Herpes simplex virus infection is sensed by both Toll-like receptors and retinoic acid-inducible gene- like receptors, which synergize to induce type I interferon production. J Gen Virol 90: 74–78.
11. Samanta M, Iwakiri D, Kanda T, Imaizumi T, Takada K (2006) EB virus-encoded RNAs are recognized by RIG-I and activate signaling to induce type I IFN. EMBO J 25: 4207–4214.
12. Onoguchi K, Onomoto K, Takamatsu S, Jogi M, Takemura A, et al. (2010) Virus-infection or 5′ppp-RNA activates antiviral signal through redistribution of IPS-1 mediated by MFN1. PLoS Pathog 6: e1001012.
13. Hale BG, Randall RE, Ortin J, Jackson D (2008) The multifunctional NS1 protein of influenza A viruses. J Gen Virol 89: 2359–2376.
14. Portela A, Digard P (2002) The influenza virus nucleoprotein: a multifunctional RNA-binding protein pivotal to virus replication. J Gen Virol 83: 723–734.
15. Buchan JR, Parker R (2009) Eukaryotic stress granules: the ins and outs of translation. Mol Cell 36: 932–941.
16. Hou F, Sun L, Zheng H, Skaug B, Jiang QX, et al. (2011) MAVS Forms Functional Prion-like Aggregates to Activate and Propagate Antiviral Innate Immune Response. Cell 146: 448–461.
17. Xu LG, Wang YY, Han KJ, Li LY, Zhai Z, et al. (2005) VISA is an adapter protein required for virus-triggered IFN-beta signaling. Mol Cell 19: 727–740.
18. Seth RB, Sun L, Ea CK, Chen ZJ (2005) Identification and characterization of MAVS, a mitochondrial antiviral signaling protein that activates NF-kappaB and IRF 3. Cell 122: 669–682.
19. Kawai T, Takahashi K, Sato S, Coban C, Kumar H, et al. (2005) IPS-1, an adaptor triggering RIG-I- and Mda5-mediated type I interferon induction. Nat Immunol 6: 981–988.
20. Meylan E, Curran J, Hofmann K, Moradpour D, Binder M, et al. (2005) Cardif is an adaptor protein in the RIG-I antiviral pathway and is targeted by hepatitis C virus. Nature 437: 1167–1172.
21. Dixit E, Boulant S, Zhang Y, Lee AS, Odendall C, et al. (2010) Peroxisomes are signaling platforms for antiviral innate immunity. Cell 141: 668–681.
22. White JP, Cardenas AM, Marissen WE, Lloyd RE (2007) Inhibition of cytoplasmic mRNA stress granule formation by a viral proteinase. Cell Host Microbe 2: 295–305.
23. Nallagatla SR, Hwang J, Toroney R, Zheng X, Cameron CE, et al. (2007) 5′-triphosphate-dependent activation of PKR by RNAs with short stem-loops. Science 318: 1455–1458.
24. Baum A, Sachidanandam R, Garcia-Sastre A (2010) Preference of RIG-I for short viral RNA molecules in infected cells revealed by next-generation sequencing. Proc Natl Acad Sci U S A 107: 16303–16308.
25. Rehwinkel J, Tan CP, Goubau D, Schulz O, Pichlmair A, et al. (2010) RIG-I detects viral genomic RNA during negative-strand RNA virus infection. Cell 140: 397–408.
26. Yang YL, Reis LF, Pavlovic J, Aguzzi A, Schafer R, et al. (1995) Deficient signaling in mice devoid of double-stranded RNA-dependent protein kinase. EMBO J 14: 6095–6106.
27. Kato H, Takeuchi O, Mikamo-Satoh E, Hirai R, Kawai T, et al. (2008) Length-dependent recognition of double-stranded ribonucleic acids by retinoic acid-inducible gene-I and melanoma differentiation-associated gene 5. J Exp Med 205: 1601–1610.
28. Yoneyama M, Fujita T (2010) Recognition of viral nucleic acids in innate immunity. Rev Med Virol 20: 4–22.
29. Malathi K, Dong B, Gale M Jr, Silverman RH (2007) Small self-RNA generated by RNase L amplifies antiviral innate immunity. Nature 448: 816–819.
30. Berlanga JJ, Ventoso I, Harding HP, Deng J, Ron D, et al. (2006) Antiviral effect of the mammalian translation initiation factor 2alpha kinase GCN2 against RNA viruses. EMBO J 25: 1730–1740.
31. Ouda R, Onomoto K, Takahasi K, Edwards MR, Kato H, et al. (2011) Retinoic acid-inducible gene I-inducible miR-23b inhibits infections by minor group rhinoviruses through down-regulation of the very low density lipoprotein receptor. J Biol Chem 286: 26210–26219.
32. Saito T, Hirai R, Loo YM, Owen D, Johnson CL, et al. (2007) Regulation of innate antiviral defenses through a shared repressor domain in RIG-I and LGP2. Proc Natl Acad Sci U S A 104: 582–587.
33. Kedersha N, Anderson P (2007) Mammalian stress granules and processing bodies. Methods Enzymol 431: 61–81.
34. Diebold SS, Montoya M, Unger H, Alexopoulou L, Roy P, et al. (2003) Viral infection switches non-plasmacytoid dendritic cells into high interferon producers. Nature 424: 324–328.
35. Gilfoy FD, Mason PW (2007) West Nile virus-induced interferon production is mediated by the double-stranded RNA-dependent protein kinase PKR. J Virol 81: 11148–11158.
36. McAllister CS, Samuel CE (2009) The RNA-activated protein kinase enhances the induction of interferon-beta and apoptosis mediated by cytoplasmic RNA sensors. J Biol Chem 284: 1644–1651.
37. Carpentier PA, Williams BR, Miller SD (2007) Distinct roles of protein kinase R and toll-like receptor 3 in the activation of astrocytes by viral stimuli. Glia 55: 239–252.
38. Barry G, Breakwell L, Fragkoudis R, Attarzadeh-Yazdi G, Rodriguez-Andres J, et al. (2009) PKR acts early in infection to suppress Semliki Forest virus production and strongly enhances the type I interferon response. J Gen Virol 90: 1382–1391.

39. Schulz O, Pichlmair A, Rehwinkel J, Rogers NC, Scheuner D, et al. (2010) Protein kinase R contributes to immunity against specific viruses by regulating interferon mRNA integrity. Cell Host Microbe 7: 354–361.
40. Min JY, Li S, Sen GC, Krug RM (2007) A site on the influenza A virus NS1 protein mediates both inhibition of PKR activation and temporal regulation of viral RNA synthesis. Virology 363: 236–243.
41. Khaperskyy DA, Hatchette TF, McCormick C (2011) Influenza A virus inhibits cytoplasmic stress granule formation. FASEB J.
42. Guo Z, Chen LM, Zeng H, Gomez JA, Plowden J, et al. (2007) NS1 protein of influenza A virus inhibits the function of intracytoplasmic pathogen sensor, RIG-I. Am J Respir Cell Mol Biol 36: 263–269.
43. Mibayashi M, Martinez-Sobrido L, Loo YM, Cardenas WB, Gale M Jr, et al. (2007) Inhibition of retinoic acid-inducible gene I-mediated induction of beta interferon by the NS1 protein of influenza A virus. J Virol 81: 514–524.
44. Gack MU, Albrecht RA, Urano T, Inn KS, Huang IC, et al. (2009) Influenza A virus NS1 targets the ubiquitin ligase TRIM25 to evade recognition by the host viral RNA sensor RIG-I. Cell Host Microbe 5: 439–449.
45. Li W, Li Y, Kedersha N, Anderson P, Emara M, et al. (2002) Cell proteins TIA-1 and TIAR interact with the 3′ stem-loop of the West Nile virus complementary minus-strand RNA and facilitate virus replication. J Virol 76: 11989–12000.
46. Iseni F, Garcin D, Nishio M, Kedersha N, Anderson P, et al. (2002) Sendai virus trailer RNA binds TIAR, a cellular protein involved in virus-induced apoptosis. EMBO J 21: 5141–5150.
47. Simpson-Holley M, Kedersha N, Dower K, Rubins KH, Anderson P, et al. (2010) Formation of antiviral cytoplasmic granules during orthopoxvirus infection. J Virol 85: 1581–1593.
48. Yoneyama M, Suhara W, Fukuhara Y, Fukuda M, Nishida E, et al. (1998) Direct triggering of the type I interferon system by virus infection: activation of a transcription factor complex containing IRF-3 and CBP/p300. EMBO J 17: 1087–1095.
49. Daly C, Reich NC (1993) Double-stranded RNA activates novel factors that bind to the interferon-stimulated response element. Mol Cell Biol 13: 3756–3764.
50. Iwamura T, Yoneyama M, Yamaguchi K, Suhara W, Mori W, et al. (2001) Induction of IRF-3/−7 kinase and NF-kappaB in response to double-stranded RNA and virus infection: common and unique pathways. Genes Cells 6: 375–388.
51. Momose F, Kikuchi Y, Komase K, Morikawa Y (2007) Visualization of microtubule-mediated transport of influenza viral progeny ribonucleoprotein. Microbes Infect 9: 1422–1433.
52. Onoguchi K, Yoneyama M, Takemura A, Akira S, Taniguchi T, et al. (2007) Viral infections activate types I and III interferon genes through a common mechanism. J Biol Chem 282: 7576–7581.
53. Brummelkamp TR, Bernards R, Agami R (2002) A system for stable expression of short interfering RNAs in mammalian cells. Science 296: 550–553.
54. Naldini L, Blomer U, Gallay P, Ory D, Mulligan R, et al. (1996) In vivo gene delivery and stable transduction of nondividing cells by a lentiviral vector. Science 272: 263–267.
55. Zufferey R, Nagy D, Mandel RJ, Naldini L, Trono D (1997) Multiply attenuated lentiviral vector achieves efficient gene delivery in vivo. Nat Biotechnol 15: 871–875.
56. Bridge AJ, Pebernard S, Ducraux A, Nicoulaz AL, Iggo R (2003) Induction of an interferon response by RNAi vectors in mammalian cells. Nat Genet 34: 263–264.
57. Jo S, Kawaguchi A, Takizawa N, Morikawa Y, Momose F, et al. (2010) Involvement of vesicular trafficking system in membrane targeting of the progeny influenza virus genome. Microbes Infect 12: 1079–1084.

Journal of Clinical Laboratory Analysis 26: 174–183 (2012)

New Sandwich-Type Enzyme-Linked Immunosorbent Assay for Human MxA Protein in a Whole Blood Using Monoclonal Antibodies Against GTP-Binding Domain for Recognition of Viral Infection

Mizuho Kawamura,[1] Akira Kusano,[2] Akiko Furuya,[2] Nobuo Hanai,[2] Hideki Tanigaki,[1] Akihito Tomita,[1] Akira Horiguchi,[3] Kyosuke Nagata,[4] Toshiko Itazawa,[5] Yuichi Adachi,[5] Yoshie Okabe,[5] Toshio Miyawaki,[5] and Hiroaki Kohno[1]*

[1]Fuji Research Laboratories, Kyowa Medex Co., Ltd., Shizuoka, Japan
[2]Tokyo Research Park, Kyowa Hakko Kirin Co., Ltd., Tokyo, Japan
[3]Department of Research and Development, Kyowa Medex Co., Ltd., Tokyo, Japan
[4]Department of Infection Biology, Faculty of Medicine, University of Tsukuba, Tsukuba, Japan
[5]Department of Pediatrics, Faculty of Medicine, University of Toyama, Toyama, Japan

Objectives: To develop a clinically significant and practical enzyme-linked immunosorbent assay (ELISA) for the detection of MxA protein in human whole blood, a biological marker of viral infection. *Design and Methods:* A sandwich ELISA suitable for the measurement of human MxA protein in whole blood was developed using mouse monoclonal antibodies (mAbs) raised against the GTP-binding domain of human MxA protein. Prior to the assay, the whole blood sample was treated with special buffer to extract the MxA protein, improve its stability, and avoid interference from hemoglobin. *Results:* This ELISA meets all the requirements for use in routine clinical assays, especially in terms of sensitivity (detection limit: 1.3 ng/ml whole blood), accuracy (recovery: 93.0–100.0%), and rapidity (<1.5 h). The present ELISA had a sensitivity of100% and a specificity of 100% for viral infection when compared to samples from healthy control and 87.1% and 90.9% when compared to samples from the bacterial infection group. *Conclusion:* We have developed a new ELISA for measuring MxA protein in human whole blood using mAbs specific for the GTP-binding domain of MxA. This ELISA has analytical performance enough for routine clinical assay and can be used in detecting the possibility of viral infection. J. Clin. Lab. Anal. 26:174–183, 2012.

Key words: bacterial infection; interferon α, high sensitivity; high stability; rapid assay

INTRODUCTION

Interferons are produced in response to viral infections and contribute to host defense by establishing an antiviral state in target cells (1,2). Directly measuring the interferon levels in plasma is technically difficult since interferon is rapidly turned over in vivo (3). Furthermore, the circulating level of interferon does not reflect the biologically active interferon effects on target cells (2,4).

The antiviral activity of the interferon is mediated by the induction of unique proteins and more than 30 different intracellular proteins are known to be induced by interferon (5). By measuring interferon-induced proteins, the presence of biologically active interferons can be detected more consistently (6). Among the interferon-induced proteins, MxA protein is remarkable for its high levels of expression that may reach 1% of the total cytosolic protein (7) and that can be specifically induced in a dose-dependent manner by interferons both in vivo and in vitro (7, 8). MxA protein is rapidly induced after interferon-treatment (1–2 h), detectable within 2–4 h after

*Correspondence to: Hiroaki Kohno, Fuji Research Laboratories, Kyowa Medex Co., Ltd., 600-1 Minami-isshiki, Nagaizumi-cho Suntoh-gun, Shizuoka Pref. 411-0932, Japan. E-mail: hiroaki.kohno@kyowa-kirin.co.jp

Received 7 August 2011; Accepted 24 February 2012
DOI 10.1002/jcla.21507
Published online in Wiley Online Library (wileyonlinelibrary.com).

interferon exposure, both in vitro and in vivo, and reaches a maximum level within 36 h (7–10). Moreover, cellular induction of MxA protein is not subject to feedback inhibition (8). Since interferons are the sole inducers of MxA protein (11), levels of MxA protein reflect the biologically active interferon present during host cell defense mechanisms. Therefore, elevated levels of MxA protein could be an indicator of endogenous interferon production mediated by an unknown viral activation (4) and so, the MxA protein levels could be used as a general marker of viral infection. It has been reported that MxA protein expression in peripheral blood mononuclear cells is a highly specific and reliable marker for interferon bioactivity (12) and that elevated leukocyte MxA protein levels reflect endogenous interferon production (13). Accordingly, the rapid determination of MxA protein from patient samples could be considered a useful test for the diagnosis of viral disease (14, 15).

Recent advances in the understanding of the structure and function of human MxA protein have revealed the presence of a GTP-binding domain and GTPase activity, which are now regarded as important factors in relation to its antiviral activity against a wide variety of viruses (16–20). Detailed elucidation of the relationship between the structure and function of MxA protein may make the accurate diagnosis of viral infectious conditions possible.

Here, we report the development of a clinically useful enzyme-linked immunosorbent assay (ELISA) for the detection of human MxA protein in whole blood, using mouse mAb that recognize a GTP-binding domain, which meet the requirements for a routine clinical assay.

MATERIALS, SAMPLES, AND METHODS

Materials and Chemicals

Reagents were obtained from the following sources: bovine serum albumin (BSA) (Miles, Inc., Kankakee, IL); 3,3′,5,5′-tetramethylbenzidine (TMBZ) solution (TMBlue, TSI Co., Milford, MA); oleamide diethanolamide (NOF Corporation, Tokyo, Japan), N-succinimidyl-6-maleimidohexanoate and 3-((3-Cholamidopropyl)dimethylammonio] propanesulfonate) (Dojindo Laboratories, Kumamoto, Japan); horseradish peroxidase (HRP) (Toyobo Co., Ltd., Osaka, Japan); BLOCK ACE® (DS pharma Biomedical Co., Ltd., Osaka, Japan); all other reagents were of analytical grade.

Clinical Samples

Whole blood samples from children who visited the outpatient clinic of Toyama University Hospital (Toyama, Japan) for acute onset fever were collected. Seventeen healthy children who had been without symptoms of infectious diseases during the previous two weeks served as controls. The study was conducted according to the ethical standards of the University of Toyama, which require informed consent from the parents of each subject.

Children with acute onset fever were subdivided into three groups according to the final diagnoses: (1) etiologically diagnosed viral infection, (2) clinically diagnosed viral infection, and (3) bacterial infection. Individuals with etiologically diagnosed viral infection were identified by positive results using the following virus-detection kits: Adenovirus GSA (Meridian Bioscience, Cincinnati, OH) for adenovirus, ROTA-ADENO DRY (Orion Diagnostica, Espoo, Finland) for rotavirus, Capilia Flu A, B (Nippon Becton Dickinson, Tokyo, Japan) for influenza viruses, and Directigen RSV (Becton Dickinson, Cockeyville, MD) for respiratory syncytial virus. Children with mild symptoms of upper respiratory infection or gastroenteritis were classified into the clinically diagnosed viral infection group. Their symptoms resolved spontaneously even though antibiotics were not used. Bacterial infections were diagnosed based on positive culture results and all the child patients with bacterial infections were treated successfully with antibiotics.

Whole blood samples were freshly prepared from EDTA anticoagulated blood. When whole blood was used for the ELISA, the sample was diluted immediately with the dilution buffer (0.1 mol/l Tris-HCl buffer [pH8.5] containing 2.5% [w/v] 3-[(3-Cholamidopropyl) dimethylammonio] propanesulfonate, 1.2% [w/v] oleamide diethanolamide, 0.1 mol/l NaCl, 4.0% [w/v] BLOCK ACE®, 0.1% [w/v] BSA, and 0.1% [w/v] NaN_3), stored at 4°C and was measured within 24 h after the collection. When the sample was stored for a long time, the diluted sample was stored at –80°C and was thawed just before ELISA assay.

Serum samples were prepared from blood allowed to clot at 37°C for 30 min, by centrifugation at 3,000 rpm for 10 min.

Preparation of MxA Protein

An expression vector pET-14b (Merck Biosciences, Darmstadt, Germany) containing full-length MxA protein-encoding cDNA was introduced into *Escherichia coli (E. coli)* cells (21), and were cultured at 37 °C for 4 h in 200 ml of LB medium containing 50 μg/ml of ampicillin, followed by the addition of 0.4 mmol/l of isopropylthiogalactoside and subsequently cultured at 37°C for 2 h.

E. coli was collected from 200 ml of the cultured broth by centrifugation at 3,000 rpm for 15 min, washed with phosphate-buffered saline (PBS), and was suspended in 20 mmol/l Tris-HCl buffer (pH7.9) containing 5 mmol/l imidazole and 0.5 mol/l NaCl, and then lysed by

ultrasonic treatment. After the suspension was centrifuged, the supernatant was discarded, and the residue was added to the binding buffer (20 mmol/l Tris-HCl buffer (pH7.9) containing 6 mol/l urea, 5 mmol/l imidazole, and 0.5 mol/l NaCl) and Ni-NTA His-Bind resin (EMD Bioscience, Inc., Milwaukee, WI) to purify full-length human MxA protein with a N-terminal His (6) tag from the *E. coli* inclusion bodies. The suspension was mixed by gentle rolling at 4°C for 2 h to bind MxA protein on the resin and the resin was recovered by centrifuge. The recovered resin was washed with the binding buffer and was eluted using 20 mmol/ml Tris-HCl buffer (pH7.9) containing 6 mol/l urea, 1 mol/l imidazole, and 0.5 mol/l NaCl to produce crude MxA protein. Using this method, 1.4 mg of MxA protein was recovered from 250 ml of the *E. coli* culture broth.

Immunization, Cell Fusion, and Cloning

BALB/C mice (six weeks old, male) were immunized with the recombinant human MxA protein. The monoclonal hybridoma cells were made by fusion with spleen cells derived from the immunized mouse and 2×10^7 P3×63-Ag.8.U1 cells, as described previously (22). Cell culture supernatants were tested for antibody activity by ELISA using a MxA protein-coated plate as described previously (22). Cells from positive wells were further selected on the basis of specificity and subclass, and were cloned twice by limiting dilution. Stable hybridoma clones were propagated as ascites tumors in BALB/C mice. Antibodies from monoclonal hybridoma cells were purified from the ascites by affinity chromatography using Protein-A Sepharose fast flow (GE healthscience Japan, Tokyo, Japan) according to the manufacturer's instructions.

The subclass of the monoclonal antibody was determined by a Zymed mouse mAb isotyping kit (Zymed Laboratories, Inc., San Francisco, CA). The dissociation constant of the antibody was determined by the method of Djavadi-Ohaniance et al. (23).

Western Blotting

One microgram of MxA protein derived from *E. coli* was fractionated by sodium dodecyl sulfate-polyacrylamide gel electrophoresis (SDS-PAGE) and then blotted on a polyvinylidene difluoride (PVDF) membrane. After blocking with a BSA solution, the membrane was incubated with 10 μg/ml of each of the purified anti-human MxA protein mAb for 2 h at room temperature. After thorough washing with PBS containing 0.1% (w/v) Tween 20, a HRP-labeled anti-mouse immunoglobulin antibody (DAKO Japan, Kyoto, Japan) was incubated at room temperature for 1 h. After thorough washing, color development was performed using the HAP-Color Development Reagent substrate solution (DAKO Japan).

Immnocytostaining

A suspension of human glioma T98G (ATCC CRL 1690) cells was dispensed in 500 μl portions to separate wells of an eight-well chamber slide (2×10^4 cells/well), stimulated with interferon α (1,000 U/ml) and cultured at 37°C. After washing with PBS, 500 μl of freshly prepared 4% (v/v) paraformaldehyde was added into each well and the cells were fixed at room temperature for 30 min.

The fixed cells were treated with 0.2% (v/v) Triton X-100 for 5 min to permeablize the cell membrane, incubated with 10% (v/v) normal horse serum for 30 min for blocking, and then with 10 μg/ml of each of the purified anti-human MxA protein mAb for 30 min at room temperature. After washing with PBS, 200 μl of fluorescein isothiocyanate (FITC)-labeled anti-mouse immunoglobulin antibody (Wako Pure Chemical Industries, Osaka, Japan) was added into each well at room temperature for 30 min in the dark. After thorough washing with PBS, the cells were sealed with glycerol on a glass slide and observed under a fluorescence microscope.

T98G infected with influenza virus were obtained from the Tokyo Institute of Technology and cultured at 37°C. The T98G were fixed with 4% (v/v) paraformaldehyde and were used for immunocytostaining using the same method as described above.

Determination of the mAb-Binding Domain

The MxA protein-encoding DNA was digested with restriction enzymes BstXI, PstI, NaeI, and BamHI following established procedures, and was subjected to in vitro transcription in the presence of T7 RNA polymerase to synthesize several mRNA samples having different lengths. Next, in vitro translation was carried out using these mRNA samples in the presence of ^{35}S-methionine to synthesize ^{35}S-methionine-labeled protein fragments that were successively shortened from the C-terminal end. The in vitro translation was carried out using reticulocyte lysate (#L416A, E. Y. Labo Inc., San mateo, CA) in accordance with the manufactured instruction manual. As a result, labeled protein fragments corresponding to amino acids 10–662, amino acids 10–468, amino acids 10–297 and amino acids 10–220, were synthesized. Each of these labeled protein fragments were allowed to react with each of the anti-human MxA protein mAb in a reaction buffer (50 mmol/l Tris-HCl buffer (pH 8.0) containing 1% (v/v) NP-40 and 0.2% (w/v) BSA) at 4°C for 1 h. The reaction solution was mixed with 40 μl of secondary antibody-labeled beads (AG-005, E. Y. Labo Inc.) and the reaction incubated at 4°C for 1 h with shaking for immunoprecipitation. The reaction mixture was subjected to

centrifugation at 10,000 × *g* at 4°C for 15 s and the precipitate obtained was separated by SDS-PAGE and the molecular weight of the precipitated protein was determined by autoradiography.

ELISA System

Sensitization of plates

KM1135-coated polystyrene 96-well microtiter plates (Maxisorp Immunoplates, NUNC, Rosklide, Denmark) were prepared as described previously (24). The plates were sealed in an aluminum-coated pack with a drying agent (Hi-sheet dry, Marutani chemical Plant & Engineering Co., Ltd., Tokyo, Japan) and stored at 4°C until use. Under these storage conditions, the sensitized plates were stable for at least 1 year.

Antibody-HRP conjugate

The KM1124-HRP conjugate was prepared as described previously (24). The average number of HRP molecules introduced per IgG molecule was 4.3.

The conjugate produced was diluted to 50 ng/ml with 50 mmol/l Bis-Tris buffer (pH 7.0) containing 0.1% (w/v) BSA, 50 mmol/l NaCl, 0.01% (w/v) 4-aminoantipyrine, 0.1% (v/v) polyoxyethylene polyoxypropylene glycol, 0.035% (v/v) Proclin 300® (Sigma-Aldrich Japan Co, Tokyo, Japan), and 100 mg/l mouse IgG (Roche Diagnostics GmbH, Mannheim, Germany), divided into 11 ml each in clear bottles and stored at 4°C until use. Under these storage conditions, the conjugate was stable for at least 1 year.

Standard preparation

For the standard in the ELISA, a recombinant MxA protein was prepared from *E. coli* cells transformed with an expression vector containing a MxA protein-encoding cDNA as described above. The recombinant MxA protein was furthermore purified by gel filtration column chromatography using Superose 12HR10/30 (GE healthscience Japan) eluted with 20 mmol/ml Tris-HCl buffer (pH7.9) containing 6 mol/l urea, 0.5 mmol/l imidazole, 0.1 mmol/l dithiothreitol, and 0.5 mol/l NaCl at 0.5 ml/min. The highly purified MxA protein was confirmed to be monomeric and homogeneous by high performance liquid chromatography (HPLC) and SDS-PAGE, respectively. Amino acid sequence analysis confirmed the highly purified protein as human MxA protein.

The protein concentration of the MxA protein was determined by the Bradford method (25) using the Bio-Rad DC Protein Assay Kit (Bio-Rad Laboratories, CA) with BSA as the standard, and was found to be 0.257 mg/ml.

The MxA protein solution was diluted to 24 ng/ml with the dilution buffer, divided into 1 ml each in a brown vial and lyophilized at –50°C for 48 h. After displacement of the atmospheric gases in the vial by N_2, the vial was sealed and the lyophilized MxA protein was stored at 4°C until use. When used in the ELISA, 1 ml of distilled water was added to the vial to resuspend the MxA protein, and the concentration of this MxA protein was determined to be 24 ng/ml.

To prepare the standards, 24 ng/mL of MxA protein was serially diluted with the dilution buffer and 0.38, 0.75, 1.50, 3.00, 6.00, 12.00, and 24.00 ng/ml of standards were prepared. The results of the ELISA were expressed in ng/ml of whole blood as determined by the standards.

Enzyme-linked immunosorbent assay

Twenty-five microliter of whole blood was diluted with 225 μl of the dilution buffer for cell lysis. One hundred microliter of the diluted sample or standard was added to each well of the antibody-coated plates and the plate was then incubated for 30 min at room temperature. After washing the plate five times with the washing buffer (PBS containing 0.05% [v/v] Tween-20), 100 μl of HRP-labeled KM1124 conjugate was added to each well, and the plate was incubated for 30 min at room temperature. After washing the plate five times with the washing buffer, 100 μl of TMBZ solution was added to each well, and the plate was then incubated for 10 min at room temperature. To stop the enzyme reaction, 50 μl of 0.5 mol/l H_2SO_4 was added, and the absorbance at 450 nm was measured with an MTP-120 plate reader (Corona Electric Co. Ltd., Tokyo, Japan).

Interference Study

Interference by lipids, direct bilirubin, indirect bilirubin, hemoglobin, and various anticoagulants was examined by the addition of the test metabolite to aliquots of whole blood. Metabolites and chemicals to be tested for interference were obtained from commercial sources at the highest purity available. Interference by lipids was tested using Intralipid® (Kabivitrum, Inc., California). Interference by heterophilic antibodies was tested using HAMA Sera® (Roche Diagnostics GmbH).

Statistical Analysis

Data are expressed as mean ± SD or median. Differences were examined by the Student's *t*-test or the Mann–Whitney *U* test. Receiver operating characteristic (ROC) analyses were done using the method of Hanley and McNeil (26). Computer analysis was performed with the Statcel package (OMS, Ltd., Saitama, Japan).

TABLE 1. Properties of Anti-MxA Monoclonal Antibodies

		Western blotting		Immunocytostaining		Immunoprecipitation				
KM No.	Type	76 kDa	30 kDa	IFNα	Inf	10–662	10–468	10–297	10–220	Kd
1122	IgG1	+	−	−	ND	ND	ND	ND	ND	
1123	IgG1	+	+	−	ND	ND	ND	ND	ND	ND
1124	IgG1	+	−	+	+	+	+	+	−	1.9×10^{-6}
1125	IgG1	+	−	−	ND	ND	ND	ND	ND	ND
1126	IgG1	+	−	+	−	+	+	+	+	1.8×10^{-6}
1127	IgG1	+	−	−	ND	ND	ND	ND	ND	ND
1128	IgG2a	+	+	−	ND	ND	ND	ND	ND	ND
1129	IgG1	+	−	ND	ND	ND	ND	ND	ND	
1130	IgG2a	+	+	−	ND	ND	ND	ND	ND	
1131	IgG1	+	+	−	ND	ND	ND	ND	ND	ND
1132	IgG2a	+	+	+	+	+	−	−	−	ND
1133	IgG1	+	+	−	ND	ND	ND	ND	ND	ND
1134	IgG2a	+	+	−	ND	ND	ND	ND	ND	ND
1135	IgG1	+	+	+	+	+	+	+	+	1.8×10^{-7}

ND, not done; IFNα, interferon α-stimulated cells; inf, influenza virus-infected cells.
+: positive result; −: negative result.

RESULTS

Mouse Hybridomas

Several hundred mouse hybridomas were screened by ELISA for the presence of antibodies against human recombinant MxA protein. Consequently, 14 mAb-producing lines, designated as KM1122~1135 were selected for expansion and used to produce ascites. mAb purified from ascites were used in all subsequent experiments to detect MxA protein employing the ELISA.

Characterization of mAb

As shown in Table 1, western blot analysis demonstrated all the mAb selected recognized the 76-kDa MxA protein. In addition, KM 1123, 1128, 1130–1135 also reacted with a 30-kDa band, a degradation product of the MxA protein. Immunocytostaining study said that KM1124, KM1126, KM 1132, and KM1135 could recognize the MxA protein from interferon α-stimulated cells but not unstimulated cells and additionally, KM1124, KM1132, and 1135 also reacted the MxA protein from the influenza virus-infected cells. The binding site of each mAb was determined based on the measured molecular weight. As a result, it was revealed that the anti-human MxA protein mAb KM1126 and KM1135 have a binding site at amino acids 10–220, KM1124 at amino acids 220–297, and KM1132 at amino acids 468–662, counting from the amino terminus of the MxA protein.

KM1124 and KM1135 were chosen for ELISA because of its binding site and reactivity against the cell induced by interferon α and viral infection. These antibodies had a suitable dissociation constant (Kd) to develop the ELISA system for measurement of MxA protein in whole blood.

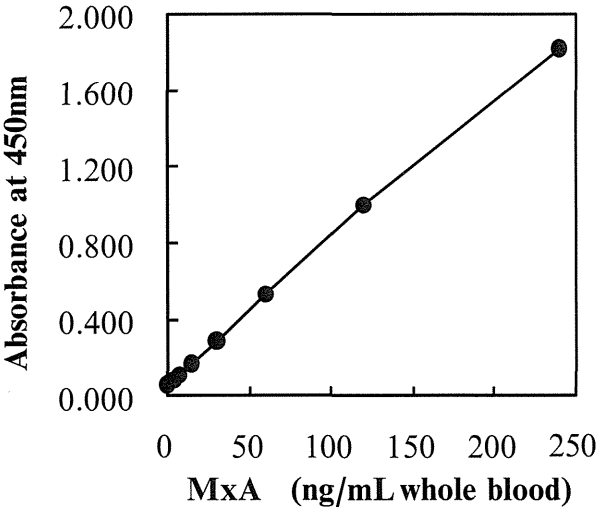

Fig. 1. Standard curve for the MxA protein-specific ELISA. Each point represents the mean of two measurements.

ELISA for Detection of MxA Protein

A sandwich ELISA for whole blood MxA protein was performed with a 96-well microtiter plate as the solid phase, KM1135 antibody as the capture antibody, KM1124-HRP conjugate as the second enzyme-labeled antibody, and TMBZ solution as the enzyme substrate. Figure 1 is a typical calibration curve generated by plotting the absorbance at 450 nm vs. the concentration of each standard.

Specificity

To confirm that the MxA protein-specific ELISA was clinically useful, T98G cells were stimulated with

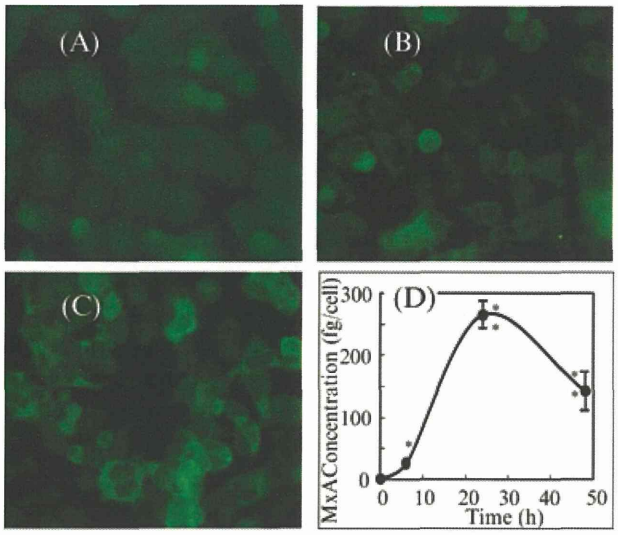

Fig. 2. Immunocytostaining and expression of MxA protein in interferon α-stimulated 98TG cells. (A) Immunocytostaining of MxA protein in 98TG cells before stimulation with interferon α, (B) after 2-h stimulation, (C) after 6-h stimulation, (D) concentration of MxA protein in 98TG cells stimulated with interferon α at 0 h. Each point represents the mean ± SD of three cultures. * and **: Significantly different from the value at 0 h, $P < 0.05$ and $P < 0.001$, respectively.

interferon α, and the MxA protein in the cell lysate was measured between 0 and 50 h. By immunocytostaining with fluorescent-labeled antibody, MxA protein was confirmed in the cytoplasm of interferon α-stimulated T98G cells (Fig. 2A, B, and C). This ELISA detected MxA protein in the cell lysate concomitant with the appearance of MxA protein in the cytoplasm of interferon α-stimulated cells (Fig. 2D).

Dilution Analysis

Whole blood samples serially diluted gave results close to linearity (Fig. 3), indicating that the assay was quantitative and confirming parallelism between the standard and whole blood.

Interference

Whole blood samples containing low (47 ng/ml), medium (105 ng/ml), and high (193 ng/ml) MxA protein concentrations were supplemented with potential interfering agents at various concentrations. There was no substantial interference from lipids up to 5 g/l (in terms of total glycerol), from hemoglobin up to 15 g/l, from direct and indirect bilirubin up to 200 mg/l, heparin up to 400 mg/l, NaF up to 4 g/l, EDTA up to 2 g/l, and sodium citrate up to 10 g/l. Human anti-mouse antibody positive serum was serially added to normal human whole blood and the whole blood was used for testing for interference

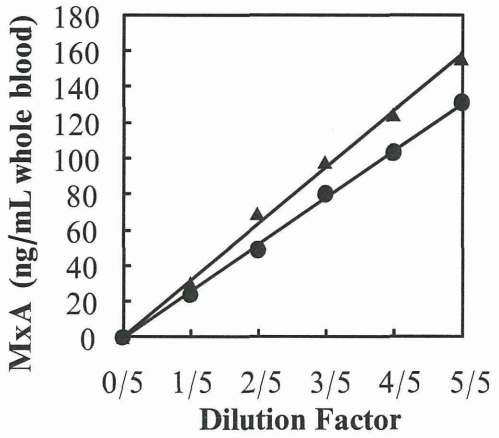

Fig. 3. Dilution curve for MxA protein in whole blood.

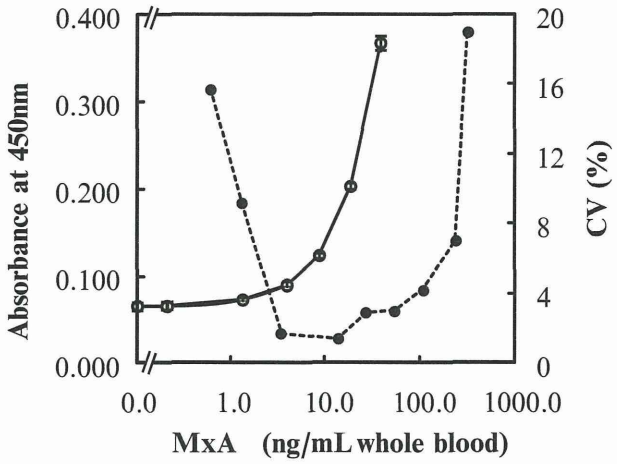

Fig. 4. Detection limit and practical assay range of MxA protein by ELISA. Each point of the detection limit represents the mean ± 2 SD of five measurements (○). Each point of the practical assay range represents the coefficients of variation (CV) value of six measurements (●).

of heterophilic antibodies. No false-positive signals were observed.

Detection Limit and Practical Assay Range of MxA Protein in Human Whole Blood

The detection limit of MxA protein in human whole blood by the ELISA was determined. Human whole blood containing MxA protein was serially diluted and used for testing. A significant difference of each serially diluted sample, compared to 0 ng/ml was confirmed by a Student's *t*-test ($n = 5$, $P < 0.001$). Figure 4 shows that 1.3 ng/ml of MxA protein in whole blood could be detected within 90 min by this assay. With the standard as the test sample, 0.13 ng/ml could be detected without pretreatment with the dilution buffer. The working range of the assay was established by calculating the coefficients of

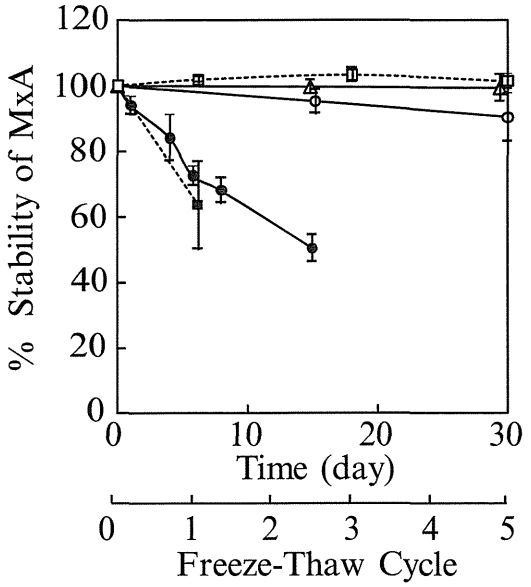

Fig. 5. Stability of MxA protein in whole blood.
–●–, stored at 4°C; –○– , treated with the dilution buffer and stored at 4°C; △ , treated with the dilution buffer and then stored at –80°C; ---■---, frozen and thawed; ---□---, treated with the dilution buffer and then frozen and thawed.

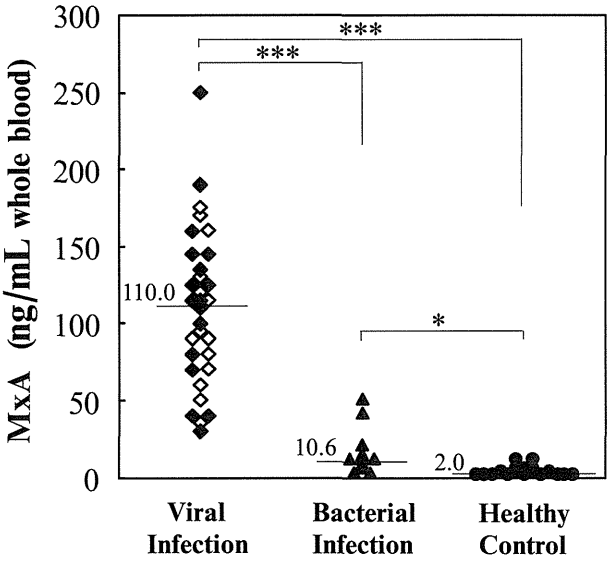

Fig. 6. MxA protein levels in whole blood of the healthy controls and patients with infection. ♦, patients with etiologically diagnosed viral infection; ◇, Patients with clinically diagnosed viral infection; ▲, patients with bacterial infection; •, healthy controls. Horizontal bars and values indicate the median for each group. $*P < 0.05$; $***P < 0.001$.

variation (CV) of each standard (range between 1.3 and 240 ng/ml) in whole blood was <10% (Fig. 4).

Assay Variation

The assay variation in the ELISA was examined using whole blood samples that contained MxA protein at three different concentrations (approximately 47 ng/ml, 105 ng/ml, and 193 ng/ml). The CV within assay and between assay were 2.0–5.5% ($n = 12$) and 2.2–7.2% ($n = 5$), respectively. To determine the analytical recovery, one volume of recombinant MxA protein (27 ng/ml and 114 ng/ml) was mixed with nine volumes of the whole blood samples containing 17, 37, and 81 ng/ml of MxA protein. Recoveries of MxA protein ranged from 93.0 to 95.0% (27 ng/ml, $n = 2$) and from 96.0 to 98.0% (114 ng/ml, $n = 2$), respectively.

Stability of MxA Protein

In this study, we used whole blood samples that had been freshly prepared. Figure 5 shows the stability of MxA protein in whole blood samples. Under refrigerated conditions, the MxA protein concentration in whole blood tended to decrease gradually. When untreated whole blood was frozen and then thawed, the MxA protein value in whole blood decreased beyond the limits of acceptability. On the other hand, when the whole blood was treated with the dilution buffer, MxA protein was stable even under refrigerated conditions. Additionally, MxA protein in diluted whole blood at –80°C was very stable for at least 3 years and freezing and thawing had no effects on the MxA protein value in the dilution buffer. Therefore, we suggest that samples for MxA protein assay are incubated with the dilution buffer immediately and then used for analysis or frozen at –80°C until needed.

Clinical Samples

The clinical performance of the present ELISA was assessed by assaying MxA protein in the whole blood of healthy controls and patients with viral infection and bacterial infection. Table 2 shows a summary of the clinical characteristics of the subjects. Significant differences in MxA protein levels, white blood cells (WBC), and C-reactive protein (CRP) were observed in the patients with viral infection compared to the healthy controls or the patients with bacterial infection. In all the groups, no significant correlations were observed between MxA protein and CRP.

Figure 6 shows the distribution of MxA protein values in the whole blood of the patients with viral infection, the patients with bacterial infection, and the healthy controls. ROC analysis was applied to the detection of the cut-off limits and then, clinical sensitivities and specificities were calculated at the cut-off limits. The MxA-specific ELISA had a sensitivity of 100% and a specificity of 100% for viral infection against healthy control and at a cut-off point of

TABLE 2. Clinical Characteristics of the Child Patients with Infection and the Healthy Control

		Viral infection			Bacterial infection	Healthy control
		Etiologically diagnosed	Clinically diagnosed	Total		
Number		17	14	31	11	18
Age	(Range)	0-10	0-6	0-10	0-6	5-11
	(Mean±SD)	2.35±2.99[c]	2.71±2.27[c]	2.52±2.66[c]	2.36±1.96[c]	7.50±1.75
Gender	(Male/Female)	6/11	8/6	14/17	8/3	12/6
MxA	(Median)	112.7[c,d]	91.7[c,d]	110.0[c,d]	10.6[c]	2.0
WBC	(Mean±SD)	10190±7175[d]	7270±1825[d]	8871±5575[d]	16352±10032	6599±1556[d]
CRP	(Median)	0.59[d]	0.49[d]	0.52[d]	7.42	0.08[d]
Final Diagnoses		RSV 10	Gastroenteritis 4		URI 5	
		Adenovirus 3	URI 10		UTI 3	
		Influenza virus A/B 3			Sepsis 2	
		Rotavirus 1			Pneumonia 1	

[a]Significantly different from the value of healthy control, $P < 0.05$.
[b]Significantly different from the value of bacterial infection, $P < 0.05$.
[c]Significantly different from the value of healthy control, $P < 0.0001$.
[d]Significantly different from the value of bacterial infection, $P < 0.0001$.
URI, upper respiratory infection; UTI, urinary tract infection.

36.7ng/ml, 87.1% and 90.9% for viral infection against bacterial infection, respectively.

DISCUSSION

The goal of this study was to develop an ELISA that met the requirements of a routine clinical assay for the measurement of MxA proteins in human whole blood.

The present ELISA is a sandwich-type assay developed using the mouse mAb KM1135 and KM1124. KM1135 recognized an epitope corresponding to the amino acids sequence of 10–220 of the human MxA protein GTP-binding domain and was used as the capture antibody. HRP-labeled KM1124 that recognized an epitope corresponding to the amino acids sequence of 221–297 was used as the secondary antibody. We selected mAb that reacted with the MxA protein GTP-binding domain, localized to the N-terminus and displayed an antivirus activity, all of which determined the specificity of the ELISA. We also checked that the mAb in this ELISA detected MxA protein in cells that was stimulated not only by interferon α but also influenza virus.

A rapid determination of MxA protein could be considered as a useful test in the diagnosis of viral disease. Towbin et al. prepared five mAb using recombinant MxA protein and they divided them into those that recognized an epitope corresponding to amino acids 1–429, and those which recognized another epitope corresponding to amino acids 430–662. They also developed a simple two-site immunometric enzyme assay with the mAb to measure MxA protein directly in blood (9). This method is simple and can measure intracellular MxA protein in whole blood, but took 20 h to perform the analysis. Oh et al. also developed a simple immunochemiluminescent assay for MxA protein (4) with the same mAb. They devised a method to reduce the time taken for analysis and to eliminate proteolytic degradation of MxA protein in whole blood lysate. However, the detection limit was 20 ng/ml in whole blood, which was insufficient to distinguish patients with viral infection from those with bacterial infection in the clinical setting.

Since MxA protein is highly susceptible to proteolysis, development of an assay system should consider eliminating any possibility of proteolytic degradation. Chieux et al. used denaturing media and heat-shock treatment to eliminate proteolytic degradation of MxA protein in blood lysate (6). In the present ELISA, we used the whole blood as a sample to measure MxA protein with the intention of developing a clinically significant and practical ELISA. As MxA protein is induced in white blood cells, the cells must be lysed before measuring MxA protein. Normally, NP-40 is used for the extraction of cytoplasmic proteins from cells. We used oleamide diethanolamide and 3-[(3-Cholamidopropyl) dimethylammonio] propanesulfonate in the dilution buffer to lyse the cells and to elute MxA protein from the cells. We checked the stability of MxA protein in various conditions by the ELISA, which detected the MxA protein GTP-binding domain of human MxA protein and found that our dilution buffer has a powerful effect on stability of the MxA protein. By using the dilution buffer for pretreatment of the whole blood, the stability of MxA protein was remarkable without the need for freezing, denaturing processes, or heat-shock treatment (6). Moreover, as freezing and thawing had also no effect on the MxA protein concentration

in the dilution buffer, samples for MxA protein measurement by the ELISA can be stored for long term at –80°C. When the whole blood was used for measuring MxA protein, high concentrations of hemoglobin were present in the sample and could interfere with the immunoreaction. Pretreatment of the whole blood with the dilution buffer also removed the interference of the hemoglobin. Additionally, the dilution buffer reduced the influence of variations in assay temperature on the assay results (data not shown). As long as we pretreated the whole blood with the dilution buffer, we could accurately measured MxA protein value in whole blood without proteolytic degradation, influence of assay condition, or interference from hemoglobin.

In this report, we demonstrated that the measurement of MxA protein in whole blood by the ELISA may be useful in the diagnosis of acute viral diseases. This assay is highly sensitive with a detection limit of 1.3 ng/ml MxA in whole blood and at 0.13 ng/ml in solution, which is sufficient to distinguish patients with viral infection from those with bacterial infections in the clinical setting. Due to the high sensitivity of the ELISA for measuring MxA protein, a sample could be pretreated and diluted 1/10 with the dilution buffer before assay. This pretreatment may remove interference from blood cell-based and plasma-based proteins and make it suitable for the routine measurement of MxA protein in human whole blood. The reproducibility and the accuracy of the ELISA are sufficient to measure MxA protein in whole blood. A total CV value of between 2.0 and 7.2% suggests this assay is very reproducible. In addition, the accuracy, as determined by the recovery of added MxA protein, is high enough for the measurement of clinical samples. This ELISA has a wide range of detection, corresponding to a clinically useful range of 1.3–240 ng/ml in whole blood. Highly purified recombinant human MxA protein was used as a standard and the use of this standard produced quantitative results in whole blood sample assays (Fig. 3).

As expected, the level of MxA protein detected in whole blood derived from patients with viral infection was significantly higher than that from healthy controls and from patients with a bacterial infection (Table 2, Fig. 6). At a cut-off point of 36.7 ng/ml, the present ELISA had a sensitivity of 87.1% and a specificity of 90.9% for viral infection against bacterial infection and the patients with viral infection were sharply distinguished from the healthy controls, that is, 100% of both a sensitivity and a specificity. The peripheral WBC count and serum CRP concentration have been used as markers to distinguish bacterial infection and viral infection. We observed that the peripheral WBC count and serum CRP concentration values were higher in the bacterial infection group compared to the viral infection group. However, the sensitivity and specificity of the MxA protein-specific ELISA was far higher than that of other markers tested, suggesting that it would be useful for the discrimination of patients with a viral infection.

It has been reported that many subjects received antibiotic treatment, despite their infections being viral in origin, and this inappropriate use of antibiotics is considered to be the main cause of the spread of multidrug-resistant bacteria (27). Several criteria have been proposed for identifying patients with bacterial infection (28–30). The present study shows that a whole blood assay for the MxA protein by the ELISA is useful for identifying the subjects whose illness is due to a viral infection. This ELISA might contribute toward a reduction in the number of unnecessary antibiotic prescriptions. However, the clinical study in this report was to assess the clinical performance of the MxA protein-specific ELISA. Further studies are necessary to establish the clinical use of the whole blood assay for MxA protein. In order to make the MxA assay more easily accessible in a clinical setting, we are pursuing the development of a rapid detection kit for MxA protein, using the same mAb and immunochromatography technology. This can detect MxA protein in whole blood within 15 min without the need for special equipment and we hope the kit will soon to be ready for clinical use.

In conclusion, we have developed a new assay, suitable for the measurement of MxA protein in human whole blood, which meets the requirements for routine clinical assay. The whole blood assay for MxA protein by the ELISA is useful for the identification of subjects who have a viral infection.

REFERENCES

1. Taylor JL, Grossberg SE. Recent progress on interferon research: Molecular mechanisms of regulation, action, and virus circumvention. Virus Res 1990;15:1–26.
2. Belardelli F. Role of interferon and other cytokines in the regulation of the immune response. APMIS 1995;103:161–179.
3. Kuzrrock R, Rosenblum MG, Sherwin AA, et al. Pharmacokinetics, single-dose tolerance, and biological activity of recombinant interferon-gamma in cancer patients. Cancer Res 1985;45:2866–2872.
4. Oh S-k, Luhowskyj S, Witt P, et al. Quantitation of interferon-induced Mx protein in whole blood lysates by an immunochemiluminescent assay: Elimination of protease activity of cell lysates in toto. J Immunol Methods 1994;176:79–91.
5. Sen CS, Lengyel P. A bird's eye view of its biochemistry. J Biol Chem 1992;267:5017–5020.
6. Chieux V, Hober D, Harvey J, et al. The MxA protein level in whole blood lysates of patients with various viral infections. J Virol Mehods 1998;70:183–191.
7. Horisberger MA. Interferon-induced human protein MxA is a GTPase which binds transiently to cellular proteins. Virology 1992;66:4705–4709.
8. von Wussow P, Jakschies D, Hochkeppel KH, Fibisch C, Penner L, Deicher H. The human intracellular Mx-homologous

protein is specifically induced by type I interferons. Eur J Immunol 1990;20:2015–2019.
9. Towbin H, Schmitz A, Jackschies D, von Wussow P, Horisberger MA. A whole blood immunoassay for the interferon-inducible human Mx protein. J Interferon Res 1992;12:67–74.
10. Ronni T, Melen K, Malygin A, Julkunen I. Control of IFN-inducible MxA gene expression in human cells. J Immunol 1993;150:1715–1718.
11. Simon A, Fäh J, Haller O, Staeheli P. Interferon-regulated Mx genes are not responsive to interleukin-1, tumor necrosis factor, and other cytokines. J Virol 1991;65:968–971.
12. Meier V, Mihm S, Ramadori G. MxA gene expression in peripheral blood mononuclear cells from patients infected chronically with hepatitis C virus treated with interferon-alpha. J Med Virol 2000;62:318–326.
13. Halminen M, Ilonen J, Julkunen I, Ruuskanen O, Simell O, Mäkelä MJ. Expression of MxA protein in blood lymphocytes discriminates between viral and bacterial infections in febrile children. Pediatr Res 1997;41:647–650.
14. Baca LM, Gems P, Kalvakolanu D, et al. Regulation of interferon-α-inducible cellular genes in human immunodeficiency virus-infected monocytes. J Leukocyte Biol 1994;55:299–309.
15. Jakschies D, Armbrust A, Clare KU, et al. Significant difference of the MxA-protein expression in human PBL of patients with viral and bacterial infections. J Interferon Res 1994;14:S124.
16. Haller O, Kochs G. Interferon-induced Mx proteins: Dynamin-like GTPases with antiviral activity. Traffic 2002;3:710–717.
17. Staeheli P, Haller O, Boll W, Lindenmann J, Weissmann C. Mx protein: Constitutive expression in 3T3 cells transformed with cloned Mx cDNA confers selective resistance to influenza virus. Cell 1986;44:147–158.
18. Zhao H, De BP, Das T, Banerjee AK. Inhibition of human parainfluenza virus-3 replication by interferon and human MxA. Virology 1996;220:330–338.
19. Schnorr JJ, Schneider-Schaulies S, Simon-Jodicke A, Pavlovic J, Horisberger MA, ter Meulen V. MxA-dependent inhibition of measles virus glycoprotein synthesis in a stably transfected human monocytic cell line. J Virol 1993;67:4760–4768.
20. Chieux V, Chehadeh W, Harvey J, Haller O, Wattre P, Hober D. Inhibition of coxsackievirus B4 replication in stably transfected cells expressing human MxA protein. Virology 2001;283:84–92.
21. Horisberger MA, McMaster G, Zeller H, Wathelet M, Dellis MG, Content J. Cloning and sequence analysis of cDNAs for interferon- and virus-induced human Mx-proteins reveal that they contain putative guanine nucleotide-binding site: Functional study of the corresponding gene promoter. J Virol 1990;64:1171–1181.
22. Kohno H, Sato S, Chiba H, et al. Monoclonal antibodies specific for 18-hydroxycortisol and their use in an enzyme immunoassay for human urinary 18-hydrocortisol for diagnosis of primary aldosteronism. Clin Biochem 1994;27:227–282.
23. Djavadi-Ohaniance L, Goldberg ME, Friguet B. Chapter 4. Measuring antibody affinity in solution. In: McCafferty J, editor. Antibody Engineering. Oxford: IRL Press; 1996. p 77–97.
24. Kohno H, Sueshige N, Oguri K, et al. Simple and practical sandwich-type enzyme immunoassay for human oxidatively modified low density lipoprotein using anti-oxidized phosphatidylcholine monoclonal antibody and anti-human apolipoprotein-B antibody. Clin Biochem 2000;33:243–253.
25. Bradford MM. Rapid and sensitive method for the quantitation of microgram quantities of protein utilizing the principle of protein-dye binding. Anal Biochem 1976;72:248–254.
26. Hanley JA, McNeil BJ. A method of comparing the areas under receiver operating characteristic curves derived from the same cases. Radiology 1983;148:839–843.
27. Huang N, Morlock L, Lee CH, Chen LS, Chou YJ. Antibiotic prescribing for children with nasopharyngitis (common colds), upper respiratory infections, and bronchitis who have health-professional parents. Pediatrics 2005;116:826–832.
28. Baker MD, Bell LM, Avner JR. Outpatient management without antibiotics of fever in selected infants. N Engl J Med 1993;329:1437–1441.
29. Baskin MN, O'Rourke EJ, Fleisher OR. 1992. Outpatient treatment of febrile infants 28 to 89 days of age with intramuscular administration of ceftriaxone. J Pediatr 120: 22–27.
30. Jaskiewicz JA, McCarthy CA, Richardson AC, et al. Febrile infants at low risk for serious bacterial infection-an appraisal of the Rochester criteria and implications for management. Febrile Infant Collaborative Study Group. Pediatrics 1994;94:390–396.

JVI
Journals.ASM.org

YB-1 Functions as a Porter To Lead Influenza Virus Ribonucleoprotein Complexes to Microtubules

Atsushi Kawaguchi,[a,b] Ken Matsumoto,[c,d] and Kyosuke Nagata[a]

Department of Infection Biology, Faculty of Medicine and Graduate School of Comprehensive Human Sciences, University of Tsukuba, Tsukuba, Japan[a]; Kitasato Institute for Life Sciences, Kitasato University, Tokyo, Japan[b]; Molecular Entomology Laboratory, RIKEN, Saitama, Japan[c]; and PRESTO, Japan Science and Technology Agency, Saitama, Japan[d]

***De novo*-synthesized RNAs are under the regulation of multiple posttranscriptional processes by a variety of RNA-binding proteins. The influenza virus genome consists of single-stranded RNAs and exists as viral ribonucleoprotein (vRNP) complexes. After the replication of vRNP in the nucleus, it is exported to the cytoplasm and then reaches the budding site beneath the cell surface in a process mediated by Rab11a-positive recycling endosomes along microtubules. However, the regulatory mechanisms of the postreplicational processes of vRNP are largely unknown. Here we identified, as a novel vRNP-interacting protein, Y-box-binding protein 1 (YB-1), a cellular protein that is involved in regulation of cellular transcription and translation. YB-1 translocated to the nucleus from the cytoplasm and accumulated in PML nuclear bodies in response to influenza virus infection. vRNP assembled into the exporting complexes with YB-1 at PML nuclear bodies. After nuclear export, using YB-1 knockdown cells and *in vitro* reconstituted systems, YB-1 was shown to be required for the interaction of vRNP exported from the nucleus with microtubules around the microtubule-organizing center (MTOC), where Rab11a-positive recycling endosomes were located. Further, we also found that YB-1 overexpression stimulates the production of progeny virions in an Rab11a-dependent manner. Taking these findings together, we propose that YB-1 is a porter that leads vRNP to microtubules from the nucleus and puts it into the vesicular trafficking system.**

In general, RNA transcripts form ribonucleoprotein (RNP) complexes with a number of RNA-binding proteins. The destiny of the RNP complexes in terms of localization, stability, and translational control is regulated by their protein constituents (16, 21, 33).

The genome of influenza type A viruses consists of eight-segmented and single-stranded RNAs of negative polarity (vRNA). vRNA exists as RNP complexes (designated vRNP) with viral RNA-dependent RNA polymerase consisting of three subunits (PB1, PB2, and PA) and nucleoprotein (NP). vRNA is transcribed into mRNA and replicated through cRNA (a full-size complementary copy of vRNA) into a large number of progeny vRNAs in the nucleus (reviewed in reference 49). The replicated vRNA is assembled into vRNP, and then the progeny vRNP interacts with M1. The vRNP-M1 complex is exported from the nucleus through the CRM1-dependent pathway mediated by the interaction of the vRNP-M1 complex with NS2 (also called NEP), which is a viral protein containing a nuclear export signal (NES) (19, 52, 54, 77). After the nuclear export, it is quite likely that the progeny vRNP accumulates in the microtubule-organizing center (MTOC) and then moves to the budding site beneath the cell surface along microtubules through Rab11a-dependent vesicular trafficking systems (28, 45). Finally, a set of eight segments of vRNA is incorporated into a progeny virion with other viral structural proteins (51, 53, 79).

The Rab11a-positive recycling endosome is important for the delivery of membranes and core polarity proteins to the lateral cell surface (reviewed in references 25, 42, and 74), leading to the construction of plasma membrane domains and epithelial cell polarity through binding to motor proteins along the cytoskeleton (75). The Rab11a-positive recycling endosome is typically located in close proximity to the nucleus and associated with the MTOC. Recent reports demonstrate that a number of viruses, including influenza virus (1, 17, 47), human cytomegalovirus (36), hantavirus (61), respiratory syncytial virus (6, 73), and Sendai virus (SeV) (9), employ the Rab11a-positive recycling endosomes during the egress. However, the targeting mechanism of cargo molecules, including influenza virus vRNP, to the Rab11a-positive recycling endosome is still poorly understood.

Since only one or two viral proteins are expressed from each segment, the virus has to hijack cellular functions/machineries consisting of numerous cellular proteins to achieve every infection process. Therefore, to understand the regulatory mechanism of the localization and intracellular transport of vRNP, identification and characterization of viral and cellular proteins involved in these processes are required. Here, we identified as a novel vRNP-interacting protein, Y-box-binding protein 1 (YB-1), a cellular protein that is involved in regulation of cellular transcription and translation (41). In the nucleus, YB-1 functions as a Y-box promoter element-binding transcription factor (34, 37, 41). However, a major portion of YB-1 localizes in the cytoplasm and regulates mRNA translation and degradation as a major component of cellular mRNA ribonucleoprotein (mRNP). A sudden translational arrest in response to a variety of stresses is accompanied by the formation of stress granules (SGs) and an increase in the number of mRNA-processing bodies (P-bodies) to reprogram gene expression posttranscriptionally (3). It is suggested that SGs are aggregates of translationally inactive mRNAs containing stalled

Received 21 February 2012 **Accepted** 24 July 2012
Published ahead of print 1 August 2012
Address correspondence to Kyosuke Nagata, knagata@md.tsukuba.ac.jp.

doi:10.1128/JVI.00453-12